Available online at www.sciencedirect.com
ScienceDirect
Ore Geology Reviews 31 (2007) 139–169
ORE GEOLOGY REVIEWS
www.elsevier.com/locate/oregeorev

Geodynamic settings and tectonic model of skarn gold deposits in China: An overview

Yan-Jing Chen [a,*], Hua-Yong Chen [b], Khin Zaw [c], Franco Pirajno [d,1], Zeng-Jie Zhang [e]

[a] Guangzhou Institute of Geochemistry, Chinese Academy of Sciences, Guangzhou 510640, China
[b] Department of Geology, Queens University, Kingston, Ontario, Canada K7L 3N6
[c] CODES ARC Centre of Excellence in Ore Deposits, University of Tasmania, Private Bag 79, Hobart, Tasmania 7001, Australia
[d] Geological Survey of Western Australia, 100 Plain Street, Perth, WA 6004, Australia
[e] Institute of Mineral Resources, Chinese Academy of Geological Sciences, Beijing 100037, China

Received 5 May 2003; accepted 21 January 2005
Available online 21 June 2006

Abstract

Seventy skarn-type gold deposits, including 1 super-large, 19 large and 24 medium-sized, are known from different geotectonic units of China. They contain a total resource of approximately 1000 t of gold (625 t in South China), and account for 20% of China's gold reserves. These skarn deposits are sited in collisional orogenic belts, fault-controlled magmatic belts and reactivated cratonic margins. All of the Chinese skarn gold provinces were affected by Phanerozoic collisional orogenesis. The timing of the metallogenic events and the spatial–temporal distribution of the Chinese skarn gold deposits indicates that they were formed during ore-forming processes linked to the transition from shortening to extension in the geodynamic evolution of a collision orogen, and not to subduction systems as is commonly advocated for porphyry copper systems around the Pacific Rim.

Keywords: Skarn gold deposit; Tectonic provinces; Orogenesis; Metallogenic timing; Continental collision; CMF model; China

1. Introduction

Skarn-type (or contact metasomatic) deposits typically result from the interaction of hot hydrothermal fluids, derived from silicate magma, and cooler sedimentary rocks. Their principal attributes, including occurrence, mineralogical compositions, major commodities (e.g., copper, iron, sulphur, lead–zinc and silver), shapes of orebodies, and genetic processes are well known (e.g., Einaudi et al., 1981; Einaudi and Burt, 1982; Meinert et al., 2000). Over the past two decades, numerous skarn-type gold deposits have been discovered all over the world, and extensively described (e.g., Torrey et al., 1986; Cameron and Garmoe, 1987; Beddoe-Stephens et al., 1987; Ewers and Sun, 1989; Wilson et al., 1990; Pirajno et al., 1991; Ettlinger et al., 1992; Johson and Meinert, 1994; Meinert et al., 1997; Meinert, 1998). Their economic importance is fully recognized (e.g., Boyle, 1979; Hu, 1982; Bache, 1987; Editorial Board of AGST, 1988; Meinert, 1989; Sillitoe, 1989; Chen et al., 1992, 1997; Zhao et al., 1992, 1997; Qiu et al., 1993; Chen, 1996).

* Corresponding author. Department of Geology, Peking University, Beijing 100871, China.
E-mail address: yjchen@pku.edu.cn (Y.-J. Chen).
[1] Department of Geology, Peking University, Beijing 100871, China.

0169-1368/$ - see front matter © 2006 Elsevier B.V. All rights reserved.
doi:10.1016/j.oregeorev.2005.01.001

Table 1
List of major skarn gold deposits in China

No	Deposit/County/ Province	Latitude/Longitude	Commodity	Size	Prod. tons	Unm. tons	Predicted tons or comment	Total tons	Ore grade	Ore Mineralogy	Major alteration	Ore-forming intrusion	Host rock	Host age	Ore age	Tectonic setting	Local structure	Data source
01	Jinping/Jinping/ Yunnan	22°52′56″/ 103°00′06″	Cu, Mo, Au	S	0.67	0.67		0.67	0.20	Cpy, Py, Apy, St, Mo, Au, El, Sp, Bn, Mt	sk, si, srp, carb, chl, ser, agl	Diorite, granite porphyry	carb shale	Pz–T	K?	Southern Yangtze Craton	Ailaoshan collision belt	Chen et al., 1997
02	Jixinnao/Gejiu/ Yunnan	23°13′12″/ 103°01′42″	Au, Cu, Pb	M			5 t Au	5.0	1.27	Cpy, Py, Apy, Gl, Sp, Au, El, Mt, Mo	sk, si, srp, carb, chl, ser, agl	Granite porphyry	carb clast	Pz–T	K?	Southern Yangtze Craton	Ailaoshan collision belt	Chen et al., 1997
03	Dulong/Maguan/ Yunnan	22°59′22″/ 104°29′30″	Sn, Zn, Au	S	0.72	0.72	Poly metals	0.72	0.18	Py, Po, Cpy, St, Cas, Bi, Bs, Mo, Sp, Apy, Bn, Gl, Au,	sk, si, ka, carb, ser, ep, chl, agl		carb shale	Pz–T	K	Southern Yangtze Craton	Shiwanda Shan orogen	Chen et al., 1997
04	Qinjia/Debao/ Guangxi	23°10′48″/ 106°39′31″	Cu, Sn, Au	S	4.3	4.3	Cu deposit	4.3	0.50	Py, Po, Cpy, St, Cas, Bi, Bs, Mo, Sp, Apy, Bn, Gl, Au,	sk, si, ka, carb, ser, ep, chl, agl	Granite porphyry	carb shale	Pz–T	K	Yangtze Craton	Shiwanda Shan orogen	Zhao et al., 1997
05	Liuhe/Hengxian/ Guangxi	22°53′10″/ 109°17′34″	Au	S			>1 t Au	>1.0	5.00	Py, Cpy, Bi, Bs, Mo, Sp, Apy, Gl, Au,	sk, phy, ka, carb, ep, chl, agl		carb shale	pz	K	Huanan Orogen	Dayao Shan orogen	Zhao et al., 1997
06	Fuzichong/Cenxi/ Guangxi	23°02′42″/ 111°11′54″	Cu, Au, Pb, Zn	S	1.5	1.5	Cu deposit	1.5	0.30	Py, Po, Cpy, Gl, Sp, Apy, Bn, Au,	sk, phy, pp, carb, agl		carb clast	Pz_2–T	K	Huanan Orogen	Dayao Shan orogen	Chen et al., 1997
07	Dabaoshan/ Qujiang/ Guangdong	24°34′05″/ 113°33′00″	Cu, Au, Pb, Zn	S	2.0	2.0	Large Cu deposit	2.0	0.51	Py, Cpy, Gl, Sp, Apy, Po, Bn, Au,	sk, phy, pp, carb, agl	Granite porphyry	carb clast	Pz_2–T	K	Huanan Orogen	Meixian basin	Chen et al., 1997
08	Baoshan/ Guiyang/Hunan	25°44′44″/ 112°42′00″	Pb, Au, Zn	M	6.8	6.5	Medium Cu deposit	6.8	0.80	Apy, Py, Sp, Gl, Cpy, Po, Au, El	sk, si, ser, chl, ep, agl, carb	Granodiorite	carb shale	P–J_1	K	Huanan Orogen	Hengyang basin on Pz orogen	Zhu, 1992
09	Kangjiawan/ Changning/Hunan	26°32′44″/ 112°36′00″	Au, Pb, Zn	L	34.0	34.0	Large Pb–Zn deposit	34.0	3.65	Apy, Py, Gl, Sp, Cpy, Po, Au, El	sk, si, ser, chl, ep, agl, carb	Dacitic porphyry	carb shale	P–J_1	K	Huanan Orogen	Hengyang basin on Pz orogen	Zhu, 1992
10	Yagongtang/ Changning/Hunan	26°33′00″/ 112°35′12″	Au, Pb, Ag	M	7.4	7.4		7.4	2.00	Apy, Py, Gl, Sp, Cpy, Po, Au, El, Ag	sk, si, ser, chl, ep, agl, carb	Granodiorite	carb shale	P	K	Huanan Orogen	Hengyang basin on Pz orogen	Zhu, 1992
11	Tianpaishan/ Qianshan/Jiangxi	28°12′00″/ 117°46′15″	Cu, Au	L	22.3	20.5	Large Cu deposit	22.3	0.12	Cpy, Apy, Py, Bn, Tth, Sp, Gl	sk, si, ser, chl, ep, agl, carb,	Granite porphyry	carb shale	Pz_2–T_2	K	Huanan Orogen	Shangyao J–K Volc basin	Zheng et al., 1983
12	Qibaoshan/ Liuyang/Hunan	28°17′27″/ 113°56′15″	Cu, Pb, Au	L	29.1	29.1	2.9 t laterite Au	32	<2.7	Apy, Py, Mt, Hm Gl, Sp, Cpy	sk, si, ser, chl, ep, agl, carb	Granite porphyry	carb clast	Pz_2–T	K	Eastern Yangtze Craton	Jiuling terrane, Jiangnan Pt_2 arc	Zheng, 1991
13	Cunqian/Gao'an/ Jiangxi	28°12′00″/ 115°07′30″	Au, Cu	M	14.8	14.8		14.8	1.00	Cpy, Py, Mt, Apy, Bn, Tth Sp, Gl, Po, Au	sk, si, ser, chl, ep, agl, carb, fl	Granodiorite	carb shale	Pz_2–T_2	K	Eastern Yangtze Craton	Jiuling terrane, Jiangnan Pt_2 arc	Zhao et al., 1997
14	Chengmenshan/ Jiujiang/Jiangxi	29°40′41″/ 115°50′00″	Cu, Au	L	69.7	69.7	Large Cu deposit	69.7	0.43	Py, Cpy, Sp, Gl, Po, Mt, Sd, Tth, Mo, Bn, Cc, Mr	sk, si, carb, chl, ep, agl	Granodiorite porphyry	carb shale	Pz_2–T_2	K	Lower Yangtze district	Daye J–K Volc basin	Pan and Dong, 1999
15	Wushan/ Ruichang/Jiangxi	29°45′49″/ 115°39′00″	Cu, Au	L	67.1		Medium Cu deposit	67.1	0.5±	Py, Cpy, Mr, Sp, Gl, Cc, Sd, Tth, Bn, Apy, Mo, Mt	sk, si, carb, chl, ep, ser	Granodiorite porphyry	carb shale	Pz_2–T_2	K	Lower Yangtze district	Daye J–K Volc basin	Pan and Dong, 1999

16	Wujia/Ruichang/ Jiangxi	29°46′49″/ 115°38′45″	Au	M	5.2	5.2		5.2	4.92	Py, Cpy, Hm, Sp, Gl, Cc, Tth, Bn, Apy, Mo, Mt	sk, si, ka, carb, chl, ep, ser	Granodiorite porphyry	carb shale	Pz_2–T_2	K	Lower Yangtze district	Daye J–K Volc basin	Chen et al., 1997
17	Jilongshan/ Yangxin/Hubei	29°48′00″/ 115°25′00″	Au, Cu	L	15.0	15.0	15.0 t Au	30.0	4.04	Cpy, Py, Bn, Au, El, Gl, Sp, Mt, Hm, Mr, Rea, Orp, Tth, Mo, Cc, Po, Rds, Smi,	sk, carb, si, chl, ep, ser, fl, phl, srp, agl	Granodiorite porphyry	carb shale	Pz_2–T_2	K	Lower Yangtze district	Daye J–K Volc basin	Pan and Dong, 1999
18	Fengshandong/ Yangxin/Hubei	29°48′33″/ 115°26′53″	Cu, Au	M	16.1	12.9		16.1	0.38	Cpy, Bn, Mt, Py, Cc, Mo, Gl, Sp	sk, si, carb, chl, ep	Granodiorite porphyry	carb shale evap	Pz_2–T_2	K	Lower Yangtze district	Daye J–K Volc basin	Pan and Dong, 1999
19	Banshan/Yangxin/ Hubei	29°49′05″/ 115°26′15″	Au, Cu	M			5 t	5.0	5.97	Cpy, Py, Mo, Bn, Cc, Tth, El, Au	sk, ka, si, ser, carb, chl	Granodiorite porphyry	carb shale evap	Pz_2–T_2	K	Lower Yangtze district	Daye J–K Volc basin	Chen et al., 1997
20	Lijiawan/ Yangxin/Hubei	29°51′16″/ 115°25′00″	Cu, Au	M	5.6	5.6	Small Cu deposit	5.62	0.82	Cpy, Py, Mo, Bn, Cc, Po, Gl, Sp, Hm, Tth, Pe, El, Wi	sk, alk, si, ser, carb, chl	Granodiorite porphyry	carb evap shale	Pz_2–T_2	K	Lower Yangtze district	Daye J–K Volc basin	Zhao et al., 1999
21	Yinshan/Yangxin/ Hubei	29°54′33″/ 115°12′30″	Pb, Zn, Au	S	3.4	3.4	Au as by-product	3.4	0.40	Py, Apy, Cpy, Gl, Sp, Au, Ag, El	sk, si, ser, chl, ep, carb, srp	Granodiorite porphyry	carb evap shale	Pz_2–T_2	K	Lower Yangtze district	Daye J–K Volc basin	Chen et al., 1997
22	Fentou/Daye/ Hubei	29°59′30″/ 115°00′05″	Au	S	1.75	1.75		1.75	9.54	Mt, Po, Py, Cpy, Hm, Sp, Au, El, Ag, Mr	sk, ka, si, chl, srp, carb, ser	Quartz diorite	carb shale	Pz_2–T_2	K	Lower Yangtze district	Daye J–K Volc basin	Zhao et al., 1999
23	Shitouzui/Daye/ Hubei	30°03′16″/ 114°58′08″	Cu, Fe, Au	M	19	19		19	0.51	Cpy, Bn, Py, Mt, Hm, Ml, Cc, Cu, Mo, Sp, Sd, Au	sk, alk, carb, phl, si, srp, ep, chl	Granite porphyry	carb shale	Pz_2–T_2	K	Lower Yangtze district	Daye J–K Volc basin	Zhao et al., 1997
24	Dabaoshan/Daye/ Hubei	30°05′27″/ 114°55′00″	Au	S			2 t	2.0	8.00	Cpy, Py, Mt, Hm, Gl, Sp, Mo, Bn, Au	sk, ka, carb, si, srp, ep, chl	Granite porphyry	carb shale	Pz_2–T_2	K	Lower Yangtze district	Daye J–K Volc basin	Chen et al., 1997
25	Jiguanzui/Daye/ Hubei	30°06′00″/ 114°54′23″	Au, Cu	L	32.5	32.5	>10 t	42.5	3.80	Cpy, Py, Mt, Bn, Cc, Au, El, Ttd, Tb, Um, Bl	sk, ka, chl, srp, carb, si	Granite porphyry, diorite	carb shale	Pz_2–T_2	K	Lower Yangtze district	Daye J–K Volc basin	Pan and Dong, 1999
26	Tonglushan/Daye/ Hubei	30°06′33″/ 114°52′30″	Cu, Au, Fe	L	69	54.4	Medium Cu deposit	69	1.15	Cpy, Bn, Py, Mt, Hm, Ml, Cc, Cu, Mo, Sp, Mr, Sd	sk, alk, carb, phl, si, srp, ep, chl	Granodiorite porphyry	carb shale	Pz_2–T_2	K	Lower Yangtze district	Daye J–K Volc basin	Zhao et al., 1999
27	Houtoushan/ Daye/Hubei	30°07′38″/ 114°56′15″	Mo, Cu, Au	S	0.62	0.62	Au as by-product	0.62	0.49	Cpy, Py, Mo, Ml, Mt, Cc, Cu, Gl, Sp, Sd	sk, ka, carb, phl, si, srp, ep, chl	Granite porphyry	carb shale	Pz_2–T_2	K	Lower Yangtze district	Daye J–K Volc basin	Chen et al., 1997
28	Xiaojiapu/ Huangshi/Hubei	30°12′33″/ 115°00′15″	Au	S			2 t	2.0	4.60	Cpy, Py, Mt, Hm, Ml, Cc, Cu, Mo, Sp, Sd, Bn, Au, El	sk, carb, si, srp, ep, chl	Granite porphyry	carb shale	Pz_2–T_2	K	Lower Yangtze district	Daye J–K Volc basin	Wu, 1992
29	Xiangzikou/ Ezhou/Hubei	30°15′16″/ 114°58′45″	FeS_2, Au	S	0.67	0.67	Au as by-product	0.67	0.17	Cpy, Py, Mt, Hm, Ml, Cc, Cu, Mo, Sp, Sd, Bn, Au, El	sk, carb, si, srp, ep, chl	Granite porphyry	carb shale	Pz_2–T_2	K	Lower Yangtze district	Daye J–K Volc basin	Wu, 1994
30	Tongkeng/Ezhou/ Hubei	30°16′22″/ 114°57′30″	Cu, Fe, Au	S	0.64	0.64	Au as by-product	0.64	0.22	Cpy, Py, Mt, Hm, Ml, Cc, Cu, Mo, Sp, Sd, Bn,	sk, carb, si, srp, ep, chl	Granite porphyry	carb shale	Pz_2–T_2	K	Lower Yangtze district	Daye J–K Volc basin	Wu, 1992

(continued on next page)

Table 1 (*continued*)

No	Deposit/County/ Province	Latitude/Longitude	Commodity	Size	Prod. tons	Unm. tons	Predicted tons or comment	Total tons	Ore grade	Ore Mineralogy	Major alteration	Ore-forming intrusion	Host rock	Host age	Ore age	Tectonic setting	Local structure	Data source
										Au, El								
31	Chensheng/ Ezhou/Hubei	30°17′27″/ 114°52′30″	Cu, Fe, Au	S	1.2	1.2	Au as by-product	1.2	0.37	Cpy, Py, Mt, Hm, Ml, Cc, Cu, Mo, Sp, Sd, Bn, Au, El	sk, carb, si, srp, ep, chl	Granite porphyry	carb shale	Pz_2–T_2	K	Lower Yangtze district	Daye J–K Volc basin	Wu, 1990
32	Anqing/Huaining/ Anhui	30°34′17″/ 116°57′30″	Cu, Au	M	7.4	7.4	Medium Cu deposit	7.4	0.16	Cpy, Py, Mt, Po, Bn, Tth, Mr, Gl, Ml, Sp, Au	sk, alk, carb, si, ser, ep, chl, agl	Granodiorite	carb shale evap	Pz_2–T_2	K	Lower Yangtze district	TongWu J–K Volc basin	Wu, 1992
33	Tongshan/Guichi/ Anhui	30°52′30″/ 117°17′09″	Cu, Au, Mo	M	6.3	6.2		6.3	0.48	Cpy, Py, Mt, Po, Au	sk, si, ep, srp, carb	Granodiorite porphyry	carb shale evap	Pz_2	K	Lower Yangtze district	TongWu J–K Volc basin	Pan and Dong, 1999
34	Huangshilao/ Tongling/Anhui	30°52′30″/ 117°50′45″	Au, Cu	M	13.5	13.5		13.5	5.79	Cpy, Py, Mt, Po, Bn, Tth, Mr, Gl, Sp, Au	sk, alk, carb, si, ser, ep, chl	Diorite	carb evap shale	Pz_2–T_2	K	Lower Yangtze district	TongWu J–K Volc basin	Wu, 1992
35	Tongguanshan/ Tongling/Anhui	30°55′38″/ 117°51′15″	Cu, Au	L	33.0	30.2	Large Cu deposit	33.0	1.44	Py, Cpy, Mt, Po, Mo, Sp, Gl, Tth, Apy, Au	sk, si, chl, ep, srp, carb, ser	Quartz diorite	carb shale evap	Pz_2–T_2	K	Lower Yangtze district	TongWu J–K Volc basin	This paper
36	Mashan/Tongling/ Anhui	30°54′47″/ 117°52′11″	Au, Cu	L	7.8	7.8	25 t Au	32.8	6.45	Po, Cpy, Py, Apy, Sd, Au, El, Sp, Mr, Mt, Mo, Bi, Cub, Tb	sk, si, srp, carb, chl, ser, tal	Quartz diorite	carb shale evap	Pz_2–T_2	K	Lower Yangtze district	TongWu J–K Volc basin	Zhao et al., 1999
37	Shizishan/ Tongling/Anhui	30°55′40″/ 117°53′08″	Cu, Au	L	46.3	36.0	Medium Cu deposit	46.3	0.30	Cpy, Py, Po, Mt, Apy, Sd, Sp, Gl, Mr, Cub, Au	sk, alk, si, srp, carb, ser, chl, ep	Quartz diorite	carb evap shale	Pz_2–T_2	K	Lower Yangtze district	TongWu J–K Volc basin	Pan and Dong, 1999
38	Baocun/Tongling/ Anhui	30°55′40″/ 117°55′25″	Au, Cu	M			5 t Au	5.0	7.00	Mt, Py, Po, Cpy, Bi, Bs, Mo, Sp, Apy, Bn, Gl, Au, El	sk, alk, si, carb, ser, ep, chl	Granodiorite	carb evap shale	Pz_2–T_2	K	Lower Yangtze district	TongWu J–K Volc basin	Zhao et al., 1999
39	Xinqiao-A/ Tongling/Anhui	30°55′44″/ 117°59′40″	Au, Cu, Fe, S	L	8.9	8.0	12 t	20.9	6.20	Py, Cpy, Apy, Mt, Gl, Sp, Po, Ttd, Wi, Bs, Bn, Tth, Au, El	sk, si, ser, carb, srp, ep, chl, ka	Quartz diorite	carb evap volc	Pz_2–T_2	K	Lower Yangtze district	TongWu J–K Volc basin	Zhao et al., 1999
40	Xinqiao-B/ Tongling/Anhui	30°55′44″/ 118°00′00″	Fe, Au, Cu	SL			105 t	105	?	Bn, Tth, Ml, Tn, Hm, Gt, Ps, Py, Po, Cpy, Mt, Gl, Sp, Au	sk, si, ser, carb, srp, ep, chl, gp, agl	Quartz diorite	carb evap volc	Pz_2–T_2	K	Lower Yangtze district	TongWu J–K Volc basin	This paper
41	Fenghuangshan/ Tongling/Anhui	30°52′30″/ 118°01′40″	Cu, Au	M	18.4	10	Medium Cu deposit	18.4	0.68	Cpy, Py, Mt, Po, Bn, Tth, Mr, Gl, Sp, Au	sk, alk, carb, si, ser, ep, chl	Granodiorite porphyry	carb evap shale	Pz_2–T_2	K	Lower Yangtze district	TongWu J–K Volc basin	This paper
42	Tongjing/ Jiangning/Jiangsu	31°46′04″/ 118°35′00″	Au, Cu	M	5.5	0.4		5.5	1.97	Mt, Py, Cpy, Bn, Au, Apy, Mr, Hm, Gl, Sp	sk, ka, na, srp, si, ser, chl, agl	Syenite diatreme	carb shale	Pz–T_2	J – K	Lower Yangtze district	NingZhen J–K Volc basin	This paper
43	Funiushan/ Jiangning/Jiangsu	32°06′00″/ 119°02′45″	Cu, Au, Fe	M	9.3	2.4	Medium Cu deposit	9.3	0.85	Mt, Py, Cpy, Bn, Au, Apy, Mr, Hm, Gl, Sp	sk, ka, na, srp, si, ser, chl, agl	Granodiorite porphyry	carb shale evap	Pz_2–T_2	J – K	Lower Yangtze district	NingZhen J–K Volc basin	This paper

44	Qixiashan/ Nanjing/Jiangsu	32°10′43″/ 118°56′15″	Pb, Zn, Au, Ag	L	26.9	26.3	2.5 t Au; large Pb–Zn mine	28.4	0.95	Gl, Sp, Py, Cpy, Apy, Ps Rds, Mr, Tth, Po, Ag, Bn	si, sk, carb, chl, ep, fl, srp, ser	Diorite	carb shale evap	$Pz–T_2$	J – K	Lower Yangtze district	NingZhen J–K Volc basin	This paper
45	Langyeshan/ Chuxian/Anhui	32°17′09″/ 118°17′30″	Cu, Au	M	8.3	7.2	Small Cu deposit	8.29	0.66	Py, Cpy, Bn, Apy, Mt, Au, Hm, Gl, Sp	sk, ka, srp, si, ser, chl, agl	Granodiorite	carb evap shale	$Pz–T_2$	J – K	Lower Yangtze district	Chuxian J–K Volc basin	This paper
46	Qianchang/Suixi/ Anhui	33°41′49″/ 116°52′10″	Fe, Au, Cu	L	8.4	8.4	>15 t Au, including Sanjia	23.4	2.38	Mt, Py, Cpy, Bn, Au, Bi, Apy, El, Ku, Mr, Po, Hm, Crk, Ld, Um, Ln	sk, ka, srp, si, ser, chl, agl	Quartz diorite–granite porphyry	carb shale evap	$Pz_2–T$	J – K	Southern NC Craton	Tan-Lu FMB	Zhao et al., 1999
47	Guilaizhuang/ Pingyi/Shandong	35°22′55″/ 117°46′40″	Au	L			>20 t Au	>20.0	4.00	Py, Mt, Cpy, Gl, Sp, Apy, Bn, Sd, Cu	sk, si, carb, ka, ser, ep, chl, agl	Granite–syenite porphyry	carb shale	Pz_1	K	Inner NC Craton	Tan-Lu FMB	Chen, 2000a
48	Yinan/Shandong	35°38′11″/ 118°26′40″	Au	M	4.8	0.4	2 t Au	6.8	12.5	Py, Mt, Cpy, Bn, Bi, Cu	sk, si, carb, ka, ser, ep, chl	Diorite–granite porphyry	carb shale	Pz_1	K	Inner NC Craton	Tan-Lu FMB	Zhao et al., 1992
49	Wangbaoshan/ Wafangdian/ Liaoning	39°40′22″/ 122°43′04″	Au, Pb, Zn	S	2.8	2.8	Small Pb–Zn deposit	2.8	2.37	Cpy, Mt, Po, Py, Mo, Au, Bn, Tth, Ml	sk, alk, si, ser, chl, ep, carb, agl	Rhyolitic porphyry	carb evap shale	Pt_1	J – K	Northern NC Craton	Tan-Lu FMB	Chen et al., 1997
50	Huatong/ Wafangdian/ Liaoning	40°02′11″/ 122°54′21″	Cu, Au	M	1.8	0.9	>4 t Au; medium Cu mine	>5	3.00	Cpy, Mt, Po, Py, Mo, Au, Bn, Tth, Ml	sk, alk, si, ser, chl, ep, carb, agl	Granite	carb evap shale	Pt_1	J – K	Northern NC Craton	Tan-Lu FMB	Rui et al., 1994
51	Yinjiagou/ Lingbao/Henan	34°12′03″/ 110°48′27″	Au, Fe, S, Mo	M	7.5	7.5	Medium S and Mo deposit	7.5	13.5	Py, Gl, Sp, Mt, Cpy, Apy, Mo, Bn, Au	sk, ka, si, carb, ser, ep, chl, agl	Granite porphyry	carb shale	Pt_2	J – K	Southern NC Craton	Huaxiong block	Chen and Guo, 1993
52	Fenghuangzui/ Pinglu/Shanxi	34°45′/111°10′	Au, Fe	S					>1.0	Py, Mt, Cpy, Gl, Sp	sk, alk, agl, chl, ep, ser.	Diorite	clast carb	$Pt_2–Pz_1$	J – K	Inner NC Craton	Taihang-shan FMB	Chen et al., 1997
53	Sijiawan/ Xiangfen/Shanxi	35°51′16″/ 111°40′00″	Au, Cu	S	3.2	2.5	Small Cu mine	3.2	2.86	Py, Mt, Cpy, Gl, Sp	sk, alk, agl, chl, ep, ser.	Monzonite porphyry	carb clast	Pz	K	Inner NC Craton	Taihang-shan FMB	Chen et al., 1997
54	Diaoquan/ Lingqiu/Shanxi	39°25′/114°14′	Cu, Au	S	4.9	4.9	MediumCu mine	4.9	0.62	Cpy, Mt, Po, Py, Mr, Mo, Tn, Au, Bn, Ml, Tth	sk, alk, si, ser, chl, ep, carb, agl	Granite porphyry	carb shale	Pz	J – K	Inner NC Craton	Taihang-shan FMB	Qin, 1996
55	Tainashui/ Lingqiu/Shanxi	39°37′05″/ 114°12′42″	Au, Fe	S	2.8	2.8		2.8	7.45	Py, Mt, Cpy, Gl, Sp	sk, alk, agl, chl, ep, ser.	Dacitic porphyry	carb shale	Pz	J – K	Inner NC Craton	Taihang-shan FMB	Chen et al., 1997
56	Shouwangfen/ Chengde/Hebei	40°45′/118°30′	Cu, Mo, Au	S			Cu–Mo deposit			Cpy, Mt, Po, Py, Mr, Mo, Tn, Bn, Ml, Tth	sk, ka, si, ser, chl, ep, carb, agl	Granodiorite	carb shale	Pz	J – K	Northern NC Craton	Yan Shan mobilized belt	Qin, 1996
57	Lanjia/ Shuangyang/Jilin	43°30′/126°10′	Fe, Au, Cu	M	7.5	7.5	11 t Au	18.5	11.0	Py, Mt, Cpy, Gl, Sp, Au, El	sk, ka, si, chl, ep, ser, agl, carb	Granite, granitic porphyry	carb	Pz	J – K	Hingan collision belt	Jiamusi block	Wei and Lu, 1994
58	Laozuoshan/ Qitaihe/ Heilongjiang	46°09′32″/ 131°27′16″	Au, Cu	L	7.4	7.4	13 t Au	20.4	7.38	Py, Mt, Cpy, Gl, Sp, Mo, Bn, Tth, Au, El	sk, ka, agl, si, chl, ep, ser, carb	Diorite porphyry	carb evap shale	Pt_1	J – K	Hingan collision belt	Jiamusi block	Wei and Lu, 1994
59	Chaobuleng/ Dongwuqi/Inner Mongol	46°28′47″/ 118°40′00″	Zn, Fe, Bi, Au	S	1.7	1.7	Large Zn deposit	>1.7	0.25	Py, Sp, Mt, Cpy, Hm, Gl, Mo, Au, Bn	sk, ka, si, chl, ep, ser, carb, agl, fl	Monzonite porphyry	carb shale	Pz	J – K	Hingan collision belt	Great Hingan arc	Rui et al., 1994
60	Sankuanggou/ Nenjiang/ Heilongjiang	50°20′37″/ 125°33′40″	Cu, Au	S	1.4	1.4	Medium Cu deposit	1.4	0.39	Py, Mt, Cpy, Gl, Sp	sk, alk, agl, chl, ep, ser	Granodiorite	carb shale	Pz	J – K	Hingan collision belt	Great Hingan arc	Rui et al., 1994

(continued on next page)

Table 1 (*continued*)

No	Deposit/County/ Province	Latitude/Longitude	Commodity	Size	Prod. tons	Unm. tons	Predicted tons or comment	Total tons	Ore grade	Ore Mineralogy	Major alteration	Ore-forming intrusion	Host rock	Host age	Ore age	Tectonic setting	Local structure	Data source
61	Heihushan/Anxi/ Gansu	42°20′/96°50′	Au, Cu, Ag	S						Py, Mt, Cpy, Hm, Gl	sk, ser, chl, carb, si		carb volc	$D–C_1$	P	Tian Shan Orogen	Bei Shan orogenic belt	Zhao et al., 1997
62	Liujiaquan/Hami/ Xinjiang	41°50′/92°20′	Au, Fe	S			1.5 t	1.5		Py, Mt, Cpy, Hm, Gl	sk, ser, chl, carb, si	Syenite porphyry	carb	$D–C_1$	P	Tian Shan Orogen	Juelue Tag $D–C_1$ arc	Zhao et al., 1997
63	Ashale/Nileke/ Xinjiang	44°11′00″/ 82°50′54″	Au, Cu	M	11	11		11	5.5	Py, Cpy, Mt, Gl, Sp, Hm, Au, El, Ml, Bn, Tth, Cc, Az, Cv	sk, si, ep, chl, ser, ka, carb, agl	Biotite granite	carb shale	$Pz_1–C_1$	P	Tian Shan Orogens	Bluhuoluo-accretion prism	Chen, 2001
64	Qiaoxiahala/ Fuyun/Xinjiang	46°50′53″/ 89°42′47″	Au, Cu, Fe						0.35–2.40	Mt, Py, Hm, Spe, Cpy, Bn, Cv, Az, Ml, Cc, Au	sk, ep., chl, carb, ka, si	Quartz diorite porphyry	carb clast volc	D_2	P	Southern Altaids	Ertix (Irtysh) belt	Li, 2002
65	Baxi (Axi)/ Ruoergai/Sichuan	33°43′30″/ 103°05′00″	Au	M	6.4	6.4	In Carlin-like Au belt	6.4	4.0	Py, Apy, Cpy, Gl, Sp, Stb	sk, si, ser, ep, chl, agl	Quartz diorite porphyry	carb shale	T_2	J	Qinling collision belt	S-Qinling foreland basin	Wen and Ji, 1996
66	Deerni/Maqin/ Qinghai	34°23′42″/ 100°07′51″	Cu, Au, Co	L	29.3	29.3	Large Cu deposit	29.3	0.53	Py, Po, Cpy, Sp, Mt, Mo, Au, Rt	sk, carb, mg, si, chl, ep, ser, fl	Biotite granite	carb shale	C–P	J	Kunlun collision belt	Animaqin orogen	Duan, 1998
67	Saishitang/Xinghai Qinghai	35°18′11″/ 99°50′14″	Cu, Au	M	17.1	17.1	Large Cu deposit	17.1	0.31	Py, Mt, Hm, Ml, Cpy, Bn, Tth, Gl, Sp	sk, si, ka, chl, ep, ser, carb	Biotite granite	carb shale	Pz–T	J	Kunlun collision belt	Animaqin orogen	Chen et al., 1997
68	Yemaquan/Golmd/ Qinghai	37°00′00″/ 91°58′41″	Cu, Au	S			Medium Cu deposit			Py, Mt, Hm, Ml, Cpy, Bn, Tth, Gl, Sp	sk, si, ka, chl, ep, ser, carb	Granodiorite	carb shale	Pz_2	J	Kunlun collision belt	Qiman Tag orogen	Chen et al., 1997
69	Kendekeke/ Golmd/Qinghai	37°01′08″/ 91°46′15″	Au, Co, Bi, Cu	L	31.2	31.2	0.07 Mt Bi, 6469 t Co	31.2	1.5–38.2	Py, Apy, Bs, Tb, Mt, Cpy, Ml, Tth, Gl, Sp	sk, si, ser, carb, chl, ep, ka	Monzonite porphyry	carb chert shale	C, O_3	J	Kunlun collision belt	Qiman Tag orogen	This paper
70	Yulong/Jamda/ Tibet	31°37′33″/ 97°47′44″	Cu, Au	L	28.6	28.6	9.5 Mt Cu	28.6	0.17	Cpy, Mo, Py, Tth, Sp, Bn, Gl, Cub, Au	sk, agl, ka, pp, phl, ep, carb, chl	Granite porphyry	carb clast	T_3	Cz	Tibet–Sanjiang Orogen	Qiangtang Block	Tang and Luo, 1995

Size abbreviations: S, small (<5 t Au); M, medium (5–20 t Au); L, large (20–100 t Au); SL, super-large (>100 t Au).

Ore mineral abbreviations: Ag, native silver; Apy, arsenopyrite; Au, native gold; Az, azurite; Bi, native bismuth; Bl, bellidoite; Bn, bornite; Bs, bismuthinite; Cas, cassiterite; Cc, chalcocite; Cpy, Chalcopyrite; Crk, crookesite; Cu, native copper; Cub, cubanite; Cv, covellite; El, electrum; Gl, galena; Gt, goethite; Hm, hematite; Ku, kusttelite; Ld, ludwigite; Ln, linnaeite; Ml, malachite; Mo, molybdenite; Mr, marcasite; Mt, magnetite; Orp, orpiment; Pe, petzite; Po, pyrrhotite; Ps, psilomelane; Py, pyrite; Py-c, colloidal pyrite; Rds, rhodochrosite; Rea, realgar; Rt, rutile; Sd, siderite; Smi, smithsonite; Sp, sphalerite; Spe, specularite; St, stannite; Stb, Stibnite; Tb, tellurbismuthite; Tn, tenorite; Ttd, tetradymite; Tth, tetrahedrite; Um, umangite; Wi, wittichenite.

Alteration abbreviations: agl, argillization; alk, alkalization; carb, carbonatization; chl, chloritization; ep, epidotization; fl, fluoritization; gp, gypsum; ka, K-alteration; mg, magnesitization; na, Na-alteration; phl, phlogopitization; phy, phyllic alteration; pp, propylitization; ser, sericitization; si, silicification; sk, skarnification; srp, serpentinization; tal, talc alteration:

Abbreviations involving tectonic setting, local structure, host rocks, and ages of host rock and ore: carb, carbonate; clast, clastic; volc, volcanic; evap, evaporite. FMB, fault-controlled magmatic belt; NC, North China Craton; Pt, Proterozoic; Pz, Palaeozoic; Mz, Mesozoic; Cz, Cenozoic; Pt_1, Palaeoproterozoic or Early Proterozoic; Pt_2, Mesoproterozoic or Middle Proterozoic; Pz, Paleozoic; Pz_1, Early Paleozoic; Pz_2, Late Paleozoic; O_3, late Ordovician; D, Devonian; C, Carboniferous; P, Permian; T, Triassic; J, Jurassic; K, Cretaceous.

Prod. tons, Produced tons; Unm. tons, unmined tons.

According to Meinert (1989), skarn deposits have yielded about 1000 t of gold worldwide, excluding China. However, at least seventy deposits (Table 1), identified as gold skarns or gold-bearing skarns including copper, iron and lead–zinc, are known in China. One of them ranks as super-large (>100 t Au), nineteen are large (20–100 t Au) and twenty-four are medium-sized (5–20 t Au). The total discovered resource, amounting to more than 1000 t Au (625 t Au in South China), accounts for 20% of China's total gold reserves (including placers). The economic and exploration importance of skarn gold deposits for China has now become well established.

Skarn (or skarn-type) gold deposits can be divided into gold only, copper–(gold), copper–iron–(gold) and lead–zinc–(gold), with gold only skarn as the most attractive exploration target (Meinert, 1989). Each compositional type has a distinctive set of characteristics and tectonic setting. The bulk of gold probably entered the skarn system during retrograde alteration, concurrent with the main stage of sulphide mineralisation.

Skarn gold deposits in China are distributed in various tectonic provinces (Fig. 1) and are hosted in rocks ranging in age from the Palaeoproterozoic to the Triassic. However, the available geochronological data indicate that ore-forming processes took place from the Permian to the Cenozoic (Table 1). The importance of the skarn gold, together with the discrepancy between the age of the host rocks and the spatial–temporal distribution of the skarn deposits, requires detailed

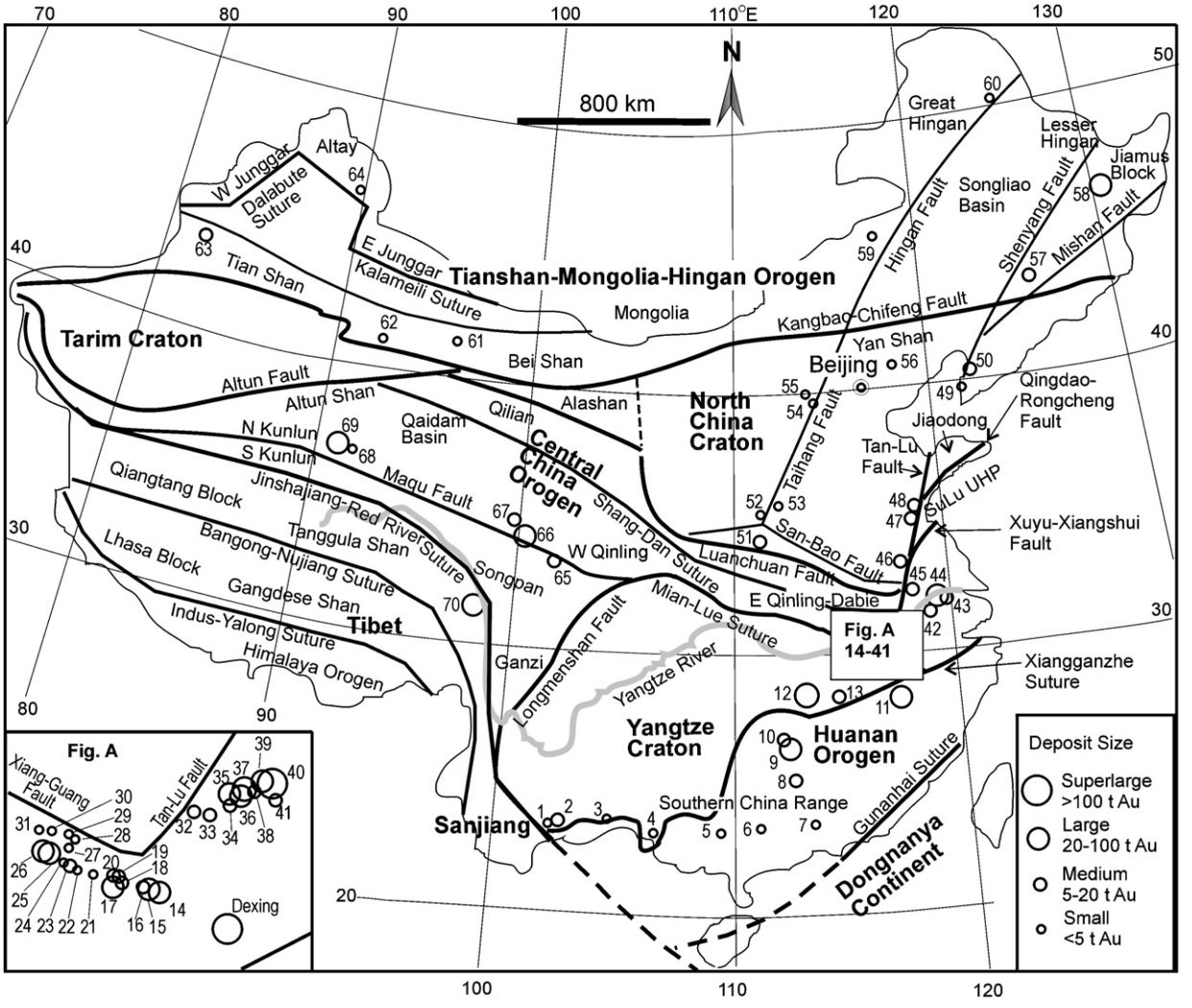

Fig. 1. Simplified map of mainland China showing tectonic provinces and distribution of 70 skarn gold deposits (numbers same as in Table 1, modified after Chen, 1996).

studies of ore genesis and of the geodynamic setting(s) of the skarn gold deposits.

In this paper we review and summarize recent advances in the study of and exploration for the skarn gold deposits in China, discuss the geodynamic environments of metallogenic belts that contain the skarn gold deposits and propose a holistic model for their genesis.

2. Review of the study of and exploration for skarn gold deposits in China

Before 1988, relatively few Chinese geologists recognized skarn gold deposits. Zhu (1953) distinguished a "contact metamorphic type", and Xie (1965) defined a "contact metasomatic type". Hu (1982), Zheng et al. (1983) and Luan (1987) also pointed out the significance of the skarn gold deposits in China. Despite these pioneering researches, the importance of skarn gold deposits in the region was not widely appreciated until the Editorial Board of AGST (1988) appealed to Chinese geologists to study and prospect for skarn gold deposits.

Since 1988, prospecting for skarn gold deposits in China has yielded great success. Many of China's skarn systems were re-evaluated and shown to contain exploitable amounts of gold. For example, the Yinjiagou gold deposit (No. 51; Table 1) was discovered by assaying samples from drill holes carried out before 1980 (HBGMR, 1989a), and is now in production. Also, some almost-closed mines such as Shouwangfen copper mine (No. 56; Table 1) and Shuikoushan lead–zinc mine (Nos. 9 and 10; Table 1) were re-evaluated and yielded encouraging results, while other deposits such as Xinqiao Cu/Fe deposit (Nos. 39 and 40; Table 1), previously considered as economically marginal, are now profitable operations. The current number of reported skarn gold deposits in China is 70 (Table 1 and Fig. 1). Their contained resource (>1000 t Au) amounts to 20% of the total gold reserve (including placers) of China. This means that skarn gold deposits are of great commercial importance to China and to the world's economy.

Based on studies of the Yinjiagou deposit (No. 51; Table 1), Chen (1990), Chen and Fu (1992), Chen and Guo (1993) reported the existence of skarn gold mineralisation in the Qinling Orogen (Fig. 1). These authors recognised three stages in the development of the deposit: (1) skarn development–alkali metasomatism, (2) sulphidisation–silicification–sericitisation and (3) carbonatisation–kaolinisation. They also demonstrated an ore–metal zonation comprising Mo–Cu → Cu–Fe–S–Au → Au–Pb–Zn → Ag (Au) → Mn (Au), and proposed that this mineralisation and related porphyry intrusions, emplaced during the Mesozoic continental collision between the Yangtze and North China Cratons (palaeocontinents) (Fig. 1). In addition, Chen et al.'s (1990a) study of the spatial relationship of the gold deposits with metamorphic carbonate strata of 2.4–1.9 Ga Liaohe Group, in the northeast margin of the North China Craton, led to the discovery of significant gold mineralisation in the Huatong skarn copper deposit (No. 50; Table 1; Fig. 1) (Rui et al., 1994). This discovery provided further impetus for skarn gold prospecting in the North China Craton, and led to the discovery of the Wangbaoshan deposit (No. 49; Table 1; Fig. 1).

The Lower Yangtze River region (Fig. 1) contains the most important skarn-type polymetallic belt in China. Skarn gold mineralisation in this region has been extensively studied (e.g., Wu, 1990, 1992, 1994; Zhao et al., 1990, 1992, 1999; Chang et al., 1991; Hu et al., 1991; Zhai et al., 1992; Gu et al., 1993, 2002; Chen et al., 1997) and recently published in English (e.g., Gu et al., 1993, 2000; Chen, 1996; Zhao et al., 1999; Pan and Dong, 1999; Zhou et al., 2000; Xu and Zhou, 2001). These authors agree that: (1) skarns formed by the interaction between fluids related to Yanshanian (Jurassic–Cretaceous) magmatism and host rocks, with metallogenesis (e.g., Cu, Au, S) occurring during the retrograde stage of skarn development and deposition of multi-phase sulphide mineralisation; (2) the orebodies may occur in the porphyritic intrusions or at the contact zones with the country rocks, and commonly form stratabound massive sulphides in the host strata; (3) Large quantities of metals or protores for later skarn-type mineralisation were made available by VHMS- and/or SEDEX-type mineralisation in Upper Palaeozoic rocks; (4) the skarn-inducing magmas originated from immature lower crust, or from mantle–crust interaction; and (5) magmatism and metallogenesis occurred during the transition from shortening to extension, during continental collision processes.

Chen (1996) and Chen and Chang (1996) reviewed the geological and geochemical parameters controlling skarn gold deposits and the geodynamic conditions that are conducive for their formation. These authors concluded that skarn deposits can be formed not only in B-subduction-related magmatic arcs (continental or oceanic), as is the case for porphyry systems, with which many skarns are intimately linked (Sillitoe, 1972), but also as a result of continetal collisions (or A-subduction system), as discussed more fully later in this paper. In the subsequent period, many geologists focused on skarn

gold deposits, especially those in the Lower Yangtze River region (Fig. 1), and this has resulted in improved understanding of their genesis and discovery of new deposits (e.g., Qin, 1996; Chang, 1997; Chen et al., 1997; Zhao et al., 1997, 1998, 1999; Wang et al., 1998; Zhang et al., 1998, 2007-this volume-a; Pan and Dong, 1999; Zhou et al., 2000, 2002a, 2007-this volume; Chen, 2000a, 2001; Xu and Zhou, 2001; Mao et al., 2002; Pirajno and Bagas, 2002; Lu et al., 2003, 2004; Zaw et al., 2007-this volume).

3. Tectonic framework and Phanerozoic collision events in China

The tectonic framework of China, from north to south, consists of four major domains: 1) the Altaids orogenic collage (including Manchurides) or Central Asian Orogenic Belt; 2) the Tarim–North China Craton or intermediate units; 3) the Tethysides; and 4) the Nipponides along the Pacific margin to the east (Figs. 2–4; Li et al., 1978; Huang and Chen, 1987; Hu et al., 1988; Hsu et al., 1988, 1990; Li and Xiao, 1996; Sengor and Natal'in, 1996; Yakubchuk et al., 2003). These domains were formed by the subduction of oceanic lithosphere, leading to continental collisions, accretion of magmatic arcs, accompanied by the emplacement of large volumes of granitic rocks (Jahn et al., 2000) and the formation of orogenic belts, incorporating fragments of pre-existing microcontinents. Within each domain, there are Precambrian blocks or terranes, subduction-related accretionary complexes, and ophiolite belts. Fig. 4 schematically illustrates the succession of geodynamic events in China, other than the Altaids, covering the time span between the Late Palaeozoic and the Cenozoic. These are discussed more fully below.

3.1. The Altaids

In China, the Altaid orogenic collage includes the Altay Shan (including Junggar Orogen), Tian Shan, the Mongolian and Hingan orogenic belts (Figs. 1–3) (Allen et al., 1992, 1993, 1995; Sengor and Natal'in, 1996). The Altaids resulted from collision between the

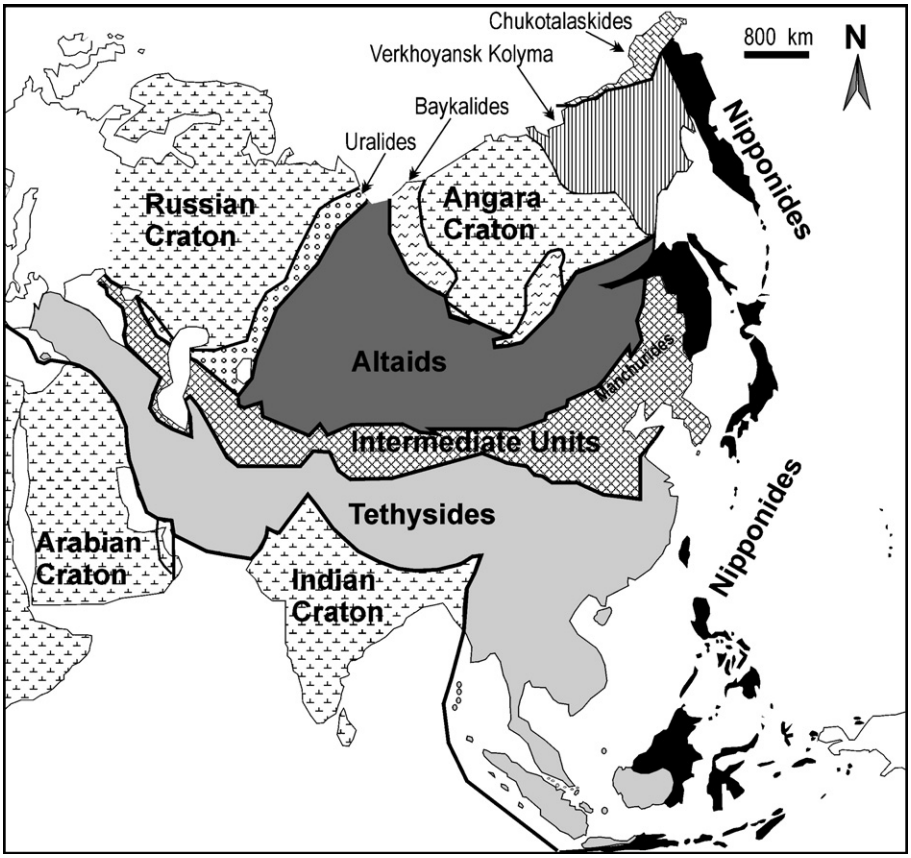

Fig. 2. Main tectonic domains of Asia (after Sengor and Natal'in, 1996).

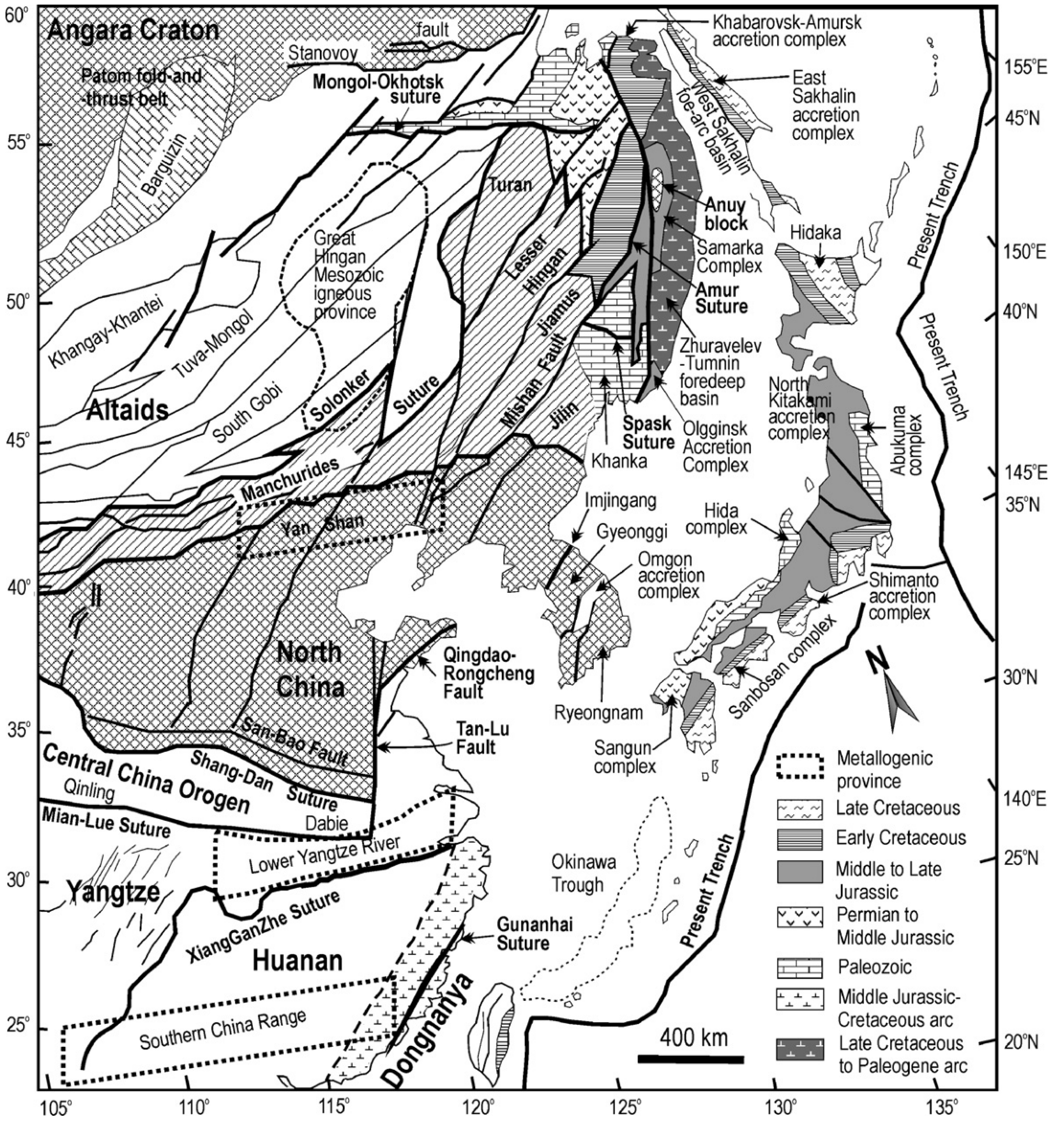

Fig. 3. Tectonic framework of Northeast China and adjacent areas (modified from Sengor and Natal'in, 1996), showing the trend of metallogenic provinces (Southern China in the Huanan orogen, the Lower Yangtze and Yan Shan) that contain skarn gold deposits in relation to the Nipponides, which overprint both the Altaids and Tethysides in East China. Other metallogenic belts are along the Tan-Lu and Taihang fault zones, which parallel the Nipponides.

Siberia Plate and the Tarim–North China Plate (including the Tarim, Alashan, and North China blocks) along the Solonker suture (Fig. 3), that progressively closed eastward from the end of Early Carboniferous to the Early Triassic (Sengor and Natal'in, 1996, and references therein). An Ar–Ar plateau age of 242±2 Ma for the metamorphism of the Hegenshan ophiolite suite supports an Early Triassic oceanic closure (Robinson et al., 1999). Nevertheless, despite the diachronous closure, the Altaids orogenic belts are generally considered to be of Hercynian age (Variscan, Late Palaeozoic 405–250 Ma).

3.2. Reactivation of the Tarim–North China intermediate units

The Tarim and North China Craton form intermediate units that separate the Altaid orogenic collage in the

north from the Tethysides belt in the south (Fig. 2). The Tarim–North China Craton comprises Archean to Palaeoproterozoic rocks, forming a metamorphic basement to a cover of unmetamorphosed Mesoproterozoic to Cenozoic rocks. Due to widespread extent of this Archean to Palaeoproterozoic metamorphic basement, the Tarim–North China Craton (Figs. 2–4) is interpreted as a stable Precambrian block, which is transected by the sinistral strike–slip Tan-Lu and Taihang faults, and is bounded by faults along the cratonic rims. The North China Craton (also known as Sino-Korean Craton; Zhang et al., 1984) is surrounded by younger orogenic belts, and parts of the Craton were reactivated during these later orogenesis. The SuLu UHP metamorphic belt, for example, was assigned to the North China Craton (e.g., Huang and Chen, 1987), but is actually a Mesozoic orogenic belt (Chen and Fu, 1992; Faure et al., 2001; Gu et al., 2002). Similarly, the Huaxiong Block, i.e. the southern margin of the North China Craton between the Luanchuan fault and San-Bao fault (Chen et al., 1990b), is now accepted as the northernmost part of the Qinling orogenic belt (Chen and Fu, 1992; Zhang et al., 1996; Sui et al., 2000). The Precambrian metamorphic basement of the Tarim–North China Craton is overlain by marine strata of Mesoproterozoic, Neoproterozoic, Early Palaeozoic and Late Palaeozoic–Triassic ages. These mainly marine rocks, although including some lacustrine coal-bearing units, indicate the existence of Proto- and Palaeo-Tethyan Seas (Huang and Chen, 1987; Xiao et al., 2000).

3.3. The Tethysides

To the south of the Tarim–North China Plate, are the giant Tethysides (Huang and Chen, 1987; Hu et al., 1988; Hsu et al., 1988, 1990; Sengor and Natal'in, 1996), that extend from the Mediterranean Sea in the west, across to southeast Asia and southeastern China (Fig. 2). The Yangtze Craton is included in the Tethysides belt because of its extensive reworking during the Tethysides Orogeny. The Yangtze Craton is a major tectonic element, joined with the Huanan Orogen along the Xiangganzhe suture (Fig. 1), also known as Jiangshan–Shaoxing suture (Zhao et al., 2001; Pirajno and Bagas, 2002). The Chinese Tethysides comprise lithofacies and sutures related to Palaeo-, Meso- and Neo-Tethyan seas, together with Precambrian blocks (e.g., the Yangtze, Qiangtang–Indochina and Lhasa blocks) (Figs. 1, 2 and 4). Local final closure time of the Palaeo-Tethyan Sea shows younging from the north to the south.

The E–W trending tract of the Kunlun/Qilian–Qinling–Dabie–SuLu orogenic belts, together forming the Central China Orogen (Figs. 1 and 4), resulted from the collision of the North China Craton with the Yangtze Craton, during Late Palaeozoic and Mesozoic (Figs. 1 and 4B). Here, continental crust is estimated to have been subducted to depths greater than 200 km (Ye et al., 2001). The Central China Orogen contains two giant sutures, which resulted from the closure, during the Late Palaeozoic and Triassic, respectively, of the Qilian–North Qinling and the Kunlun–South Qinling Oceans.

The Qilian–North Qinling Ocean is recorded by ophiolitic associations along the boundary fault belts between the Qaidam block and Qilian mountains (Li et al., 1978; Li and Xiao, 1996; Yin and Nie, 1996), the Shang–Dan suture between the northern and the southern Qinling orogenic belts (Li et al., 1978; Hu et al., 1988; Chen and Fu, 1992; Zhang et al., 1996; Hacker et al., 1996), the Guishan–Meishan fault separating the southern and northern Tongbai belts (Hu et al., 1988; Chen and Fu, 1992; Kroner et al., 1993; Zhai et al., 1998), the Xiaotian–Mozitan fault between the southern and northern Dabie Shan (Hu et al., 1988; Liu et al., 1996), and the Qingdao–Rongcheng fault in eastern Shandong (Yin and Nie, 1996; Hu et al., 1997) (Fig. 4A and B). Orogenesis related to these sutures is largely masked by the later Triassic events related to closure of the Kunlun–South Qinling Ocean (below).

The Kunlun–South Qinling Ocean is now represented, from the west to the east, by the boundary of the northern Kunlun and central Kunlun terranes (Li and Xiao, 1996), the boundary of the western Qinling and Sonpan–Ganzi complex (Zhou and Graham, 1996), the Mianxian–Lueyang ophiolite belt (Meng and Zhang, 1999; Lai et al., 2000), the Xiangfan–Guangji fault (Liu et al., 1996), and the Xuyi–Xiangshui fault (Yin and Nie, 1996; Hu et al., 1997) (Figs. 1 and 4B). Destruction of oceanic lithosphere, is now recorded by the Jinshajiang–Red River fault zones (Huang and Chen, 1987; Sengor and Natal'in, 1996; Yin and Nie, 1996; Wang et al., 2000; Lin et al., 2001), the Songpan–Ganzi fold belt (Zhou and Graham, 1996), the Xiangganzhe and the Gunanhai suture (Hsu et al., 1988, 1990; Sengor and Natal'in, 1996), were followed by Triassic collisions between the Kunlun Terrane, Qiangtang–Indochina Block, Yangtze Craton, Huanan Orogen and the hypothetical Dongnanya Continent (Figs. 1, 3 and 4). These collisions, which induced extreme crustal shortening and thickening over most of mainland China, were defined as the Indosinian Orogeny (Huang and Hsu, 1936; Zhao,

1986, and references therein). Hsu (1981) consequently suggested that South China (including the Yangtze Craton, Huanan Orogen and coastal southeastern China) is a Mesozoic thin-skinned orogenic belt, rather than a "South China Platform" (Huang, 1978). The Lower Yangtze River district (Fig. 3) is now regarded as the foreland fold-and-thrust belt of the Qinling–Dabie Mountains (Hacker et al., 1996; Liu et al., 1996;

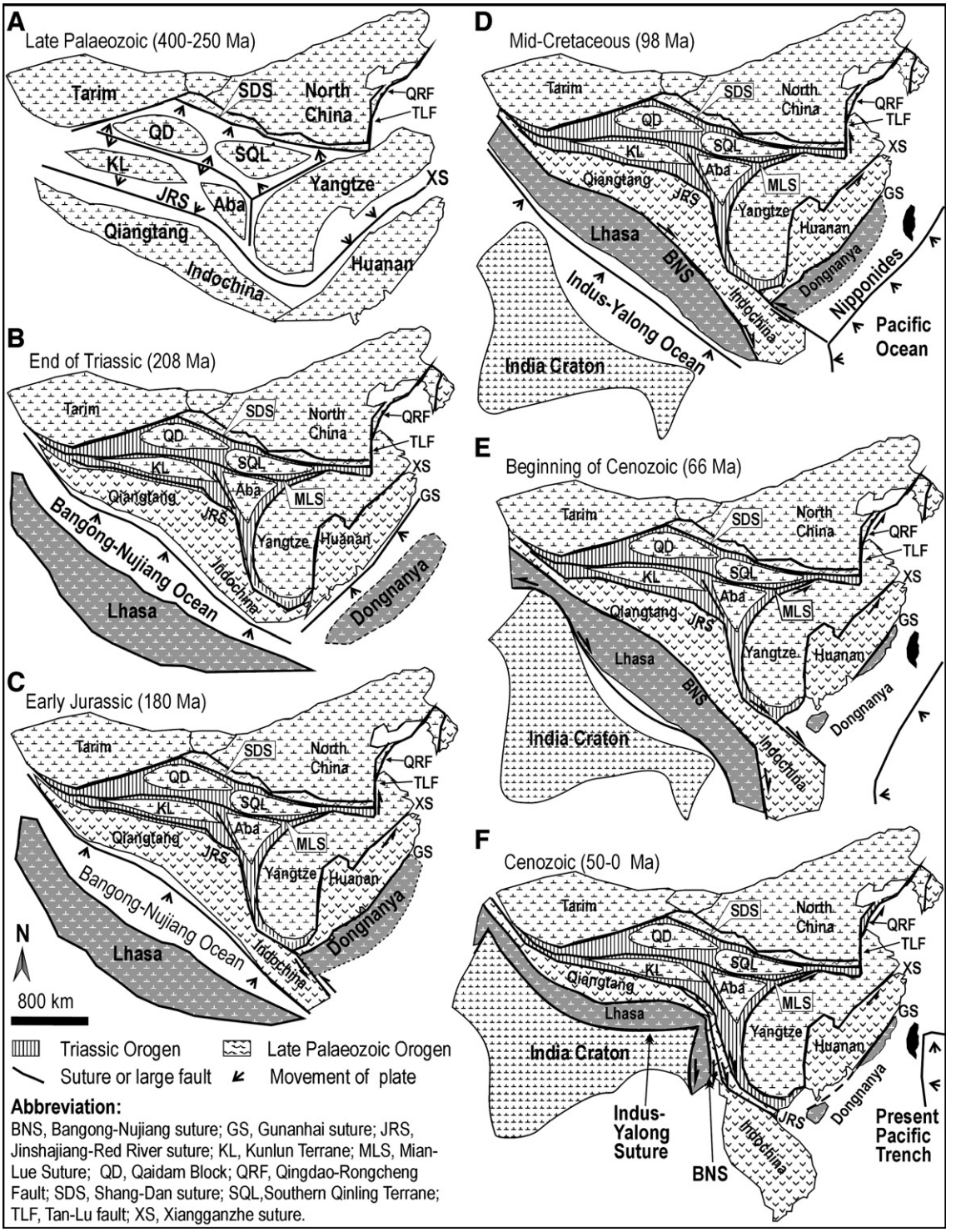

Lin et al., 2001; Gu et al., 2002, 2007-this volume) that has underwent post-shortening extension (Chen, 1990, 1998a,b; Chen and Fu, 1992). This extension, together with coeval back-arc extensions, resulting from the oceanic subduction of the Pacific Plate to the east, the Bangong–Nujiang Plate to the south and the Mongol–Okhotsk Plate to the north (see below), all of which controlled the development of eastern China during the Yanshanian Orogeny (Wong, 1927, 1929).

In the Cretaceous (ca. 98 Ma), closure of the Bangong–Nujiang Ocean (Li and Xiao, 1996; Yin and Nie, 1996) caused orogenesis and, following development of a new subduction zone, post-shortening extension (Fig. 4B, C and D). Subsequently (66–50 Ma), the India microcontinent collided with the Eurasia continent along the Indus–Yalong Zangbo suture, thereby closing the Neo-Tethyan Sea (Fig. 4D, E and F). This resulted in mountain-building of the Himalayan Orogen, uplift of the Tibet Plateau and various styles of Cenozoic deformation, such as the eastward escape tectonics, in southwestern China.

3.4. The Nipponides

The Nipponides were caused by the interaction between the Eurasian and the Pacific Plates (Sengor and Natal'in, 1996). This interaction is mainly characterized by westerly dipping subduction of the Pacific Plate. In China, only the northeasternmost area and the island of Taiwan can be assigned to the Nipponides (Figs. 2–4), but again, considerable tectonic reworking and magmatic activity in eastern China can be ascribed to the effects of the Nipponides Orogeny. In northeastern China, the Nipponides began their evolution as a circum-Pacific structure that comprises the Hingan–Okhotsk active continental margin, the Great Hingan magmatic province and other tectonic units (Fig. 3), and terminated it as a final event overprinting the Altaids (including Manchurides). The Mongol–Okhotsk Ocean was consumed by subduction during the Mesozoic and was finally closed in the Cretaceous–Palaeogene transition. The Amur suture marks the southeastern boundary of the Hingan–Okhotsk active continental margin (Fig. 3). In the Early Cretaceous, the Anuy microcontinent collided with the Hingan–Okhotsk active continental margin, thereby closing the Amur Ocean and resulting in granitic intrusions (135–105 Ma) and the Samarka accretionary complex (Fig. 3). The Hingan–Okhotsk active margin (Shao et al., 1995) and Amur suture are cut by the northeast-trending left-lateral Mishan strike–slip fault that horsetails away from the Tan-Lu fault system (Xu and Zhu, 1994; Figs. 1 and 3) and functioned as an Early Cretaceous transcurrent fault. Mesozoic orogenesis related to palaeo-Pacific Plate subduction, following closure of the Solonker Ocean, superimposed on the Altaids orogenic belts, such that Northeast China appears to be a Mesozoic rather than Palaeozoic orogenic district.

3.5. Discussion

The Phanerozoic Orogens in China can be divided into Late Palaeozoic (Hercynian), Mesozoic (Indosinian–Yanshanian) and Cenozoic (Himalayan) according to the timing of the final, most-intensive collision event. East China (including the eastern portion of the Central China Orogen) is largely a Mesozoic orogenic area, except for the island of Taiwan, where orogenesis is still ongoing. Northwest China (the western parts of Chinese Altaids) is a Hercynian orogenic area, the western part of the Central China Orogen is a Mesozoic orogenic

Fig. 4. Cartoons showing tectonic frameworks and the sequence of geodynamic events in China that formed or affected the Intermediate units (Tarim–North China), the Tethysides, and Nipponides (see also Figs. 2 and 3), between the Late Palaeozoic and the Cenozoic. (A) Opening, spreading and northward subduction of the Paleo-Tethyan Sea (Late Palaeozoic to Triassic) resulted in development of the Qilian–North Qinling Mountains and breakup of the Southern Qinling and Aba blocks from the Yangtze Craton. (B) The Paleo-Tethyan Sea finally closed when the Qiangtang–Indochina and Huanan blocks collided northwards with the Kunlun Terrane, the Aba Block and the Yangtze Craton at the end of Triassic, resulting in collision orogenies in central, southern and southeastern China areas. (C) The hypothetical Dongnanya Continent collided with the Huanan Orogen, resulting in shortening and sinistral strike–slip in East China; the northeastwards subduction of the Bangong–Nujiang Ocean (Meso-Tethyan Sea) produced back-arc extension firstly in western portion of the Central China Orogen, and then in the whole of China after the Dongnanya–Huanan continental collision reached its peak activity. (D) Low-angle northwestward subduction of the Palaeo-Pacific plate resulted in the inception of the Nipponides orogeny (e.g. Taiwan Island) and subsequent orogenic overprinting of the Tethysides in southeastern China; the Lhasa Block collided with Qiangtang–Indochina Block, the Meso-Tethyan Sea closed, and the back-arc extension ended in the whole of China. (E) During 66–50 Ma, the India Craton and the Eurasia Continent sutured, resulting in eastward closure of the Neo-Tethyan Sea (Indus–Yalong Ocean) and clockwise rotation and strike–slip escape of the Lhasa and Qiangtang blocks. (F) The India Craton is underthrust beneath the Eurasia Continent, resulting in crustal shortening and uplift of the Tibet–Sanjiang orogenic area, and causing extensive far-field uplift of the western part of the Central China Orogen, the Tian Shan and Altay orogens; dextral strike–slip and clockwise escape occurred in the Sanjiang Orogen, and sinistral strike–slip and anti-clockwise escape occurred in the eastern portion of the Central China Orogen and its adjacent areas; back-arc extension caused by the north and west-directed subduction of the Pacific plate, resulted in thinning and extension of the East China; the Dongnanya Continent became a basin and was submerged in the present-day South China Sea.

belt, and Southwest China, namely the Tibet–Sanjiang region (including the Qiantang–Indochina and Lhasa blocks and the Himalaya Mountains), is a Cenozoic orogenic region. In conclusion, although the Mesozoic–Cenozoic tectonic evolution of eastern China may have been affected by the Pacific Plate subduction (Chen, 1986; Hu et al., 1988, 1997; Yin and Nie, 1996; Wang et al., 1998; Zhou et al., 2002a), the Orogens of eastern China did not develop from the subduction of the Pacific Plate (except for the island of Taiwan).

4. Distribution and tectonic setting of skarn gold deposits in China

The Chinese skarn gold deposits, listed in Table 1, are contained in various lithotectonic units within ten metallogenic provinces (Fig. 1; Table 1): (1) Qiangtang Block (Tibet–Sanjiang region) with the Yulong deposit (No. 70); (2) southern margin of the Yangtze Craton (northern Ailaoshan–Dayaoshan region) with deposits 1 to 4 and 12 to 13; (3) Huanan Orogen (Nos. 5 to 11); (4) The eastern part of the Yangtze Craton (Lower Yangtze River region; Nos. 12 to 45); (5) Central China Orogen (Nos. 65 to 69 and 51); (6) Tan-Lu fault zone (Nos. 45 to 50); (7) Taihang fault zone (Nos. 52 to 55); (8) Yan Shan (Nos. 49 and 56); (9) Hingan Orogen (northeastern China; Nos. 57 to 60); and (10) Tian Shan–Altay orogenic belts (North Xinjiang; Nos. 61 to 64). The largest and economically most important skarn deposits are in the Yangtze Craton, Huanan Orogen and Central China Orogen (Fig. 1).

The tectonic settings of skarn gold mineralisation in China comprise: (1) continental collisional Orogens, (2) intracontinental fault-controlled magmatic belts, and (3) reactivated cratonic margins. The intersections of two or more of these environments, such as in the Lower Yangtze River region (Fig. 1), appear to be particularly favorable for the formation of skarn gold deposits.

4.1. Continental collisional orogenic belts

Collisional orogenic belts in China all contain skarn gold deposits (Table 1). The Tibet–Sanjiang orogenic belt hosts the Yulong porphyry Cu–(Mo–Au) deposits and a group of porphyry or porphyry–skarn copper–gold systems (Rui et al., 1984; Chen et al., 1997; Zhao et al., 1997; Hou et al., 2007-this volume). Although formerly regarded as a porphyry copper belt, a typical porphyry–skarn copper–gold belt, or porphyry copper skarn system as classified by Meinert (1989), the Tibet–Sangjiang region may be an important skarn gold belt. The Central China Orogen, contains the Baxi, Deerni, Saishitang, Yemaquan, Kendekeke (Nos. 65 to 69) and Yinjiagou deposits (No. 51, also at the south margin of North China Craton); the Tian Shan–Altay orogenic belt contains four skarn gold deposits (Nos. 61 to 64); the Hingan orogenic belt hosts the Chaobuleng (No. 59), Laozuoshan (No. 58), Sankuanggou (No. 60) and Lanjia (No. 57) deposits. The Huanan Orogen contains the deposits 5 to 11 (Table 1; Fig. 1), the collisional zone between the Qiangtang–Indochina block and the Yangtze Craton (Fig. 4A and B) includes deposits Nos. 1 to 4 and is highly prospective for granitoid-related skarn-type gold deposit; the richly endowed Lower Yangtze River region (eastern Yangtze Craton, Nos. 12 to 45), which is now interpreted as the foreland belt of the Dabie Orogen (e.g., Yin and Nie, 1996; Zhou et al., 2000; Lin et al., 2001); and the Huanan Orogen (Nos. 5-11; Hsu, 1981; Sengor and Natal'in, 1996).

4.2. Intracontinental fault-controlled magmatic belts

The Taihang and Tan-Lu fault zones (Fig. 1; Xu and Zhu, 1994) are examples of intracontinental fault-controlled magmatic belts in the North China Craton. They trend NNE or NE and are nearly perpendicular to collisional orogenic belts, such as the Qinling–Dabie and the Mongolia–Hingan Orogens (Figs. 1 and 3). Following the Mesozoic collision between the Yangtze and the North China Cratons, these fault zones also accommodated intracontinental extension and emplacement of large volumes of intermediate and felsic magmas that are associated with skarn-type metallic deposits, including gold-bearing skarns. Deposits Nos. 45 to 50 and 57 to 58 (Fig. 1; Table 1), and the Xi'nancha porphyry–skarn gold–copper deposit (38 t Au, 0.18 Mt Cu) (Zhou et al., 2002a) are present along the Tan-Lu fault-controlled magmatic belt and its northern extension (Shenyang fault). Along the Taihang fault-controlled magmatic belt, skarn gold deposits include the Fenghuangzui, Sijiawan, Diaoquan, and Tainashui (Nos. 52 to 55) deposits (Fig. 1), and along its northern extension (i.e. the Hingan fault) are the Chaobuleng (No. 59) and Sankuanggou (No. 60) skarn gold and the Duobaoshan porphyry Cu–Au (73 t Au) deposits.

4.3. Reactivated cratonic margins

During the Phanerozoic collisions, ancient cratonic margin sequences were affected by magmatism that produced skarn gold deposits. For instance, the southern margin of the Yangtze Craton, was involved in collisions along the Jinshajiang–Red River geosuture in the Late Triassic, and hosts the Jinping, Jixinnao, Qinjia and Liuhe

skarn gold deposits (Nos. 1 to 4; Table 1), together with the Dulong and Kafang skarn gold deposits (not shown) (Zhao et al., 1997) and the well-known Gejiu skarn tin system (Song, 1994). Similarly, the eastern margin of the Yangtze Craton (the Lower Yangtze River region), one of the most important skarn gold belt in China, with more than 30 deposits (Nos. 12 to 45, Fig. 1), was intensely reactivated in the Mesozoic.

Along the southern margin of the North China Craton, there are skarn gold deposits such as the important Yinjiagou (No. 51). These Yanshanian deposits are hosted in the Mesoproterozoic–Neoproterozoic carbonate–clastic lithofacies developed in a marginal basin of the North China Craton (Chen et al., 2000b). At the northern margin (the Yan Shan region) of the North China Craton (Figs. 1 and 3), are the Huatong (No. 50) and Shouwangfen (No. 56) deposits hosted in the Proterozoic or Palaeozoic evaporite–carbonate–clastic lithofacies (Table 1).

As indicated previously, all of the above cratonic margins underwent reactivation due to Late Palaeozoic, Mesozoic and Cenozoic collisional orogenesis. Indeed, some workers regard these marginal tracts as orogenic belts in their own right. For example, the Huaxiong block, enclosed by the San–Bao Fault and the Luanchuan Fault (Figs. 1 and 3), and which hosts the above-mentioned Yingjiagou skarn gold deposit, is regarded as part of the Qinling Orogen (Chen and Fu, 1992; Zhang et al., 1996; Yuan, 1996; Hacker et al., 1996; Sui et al., 2000; Wang et al., 2001). Likewise, the Yan Shan region (Figs. 1 and 3), the type locality of the Yanshanian Orogeny (Wong, 1927, 1929), is now interpreted in terms of the deformation that resulted from the collision of the Siberia and North China Plates during the Mesozoic closure of the Mongol–Okhotsk Ocean (Davis et al., 1996).

5. Timing of skarn gold metallogenesis in China

In order to constrain the metallogenic timing of skarn gold deposits in the various tectonic provinces and orogenic belts, and due to the paucity of isotopic ages from ore minerals, we utilise isotopic ages obtained from their associated intrusions, or other related intrusions. We discuss below the geochronology of skarn metallogeny in the Altaids in Northwest China, the Tibet–Sanjang Orogen in Southwest China, and the Mesozoic orogenic belts of East and Central China.

5.1. Northwest China: Late Palaeozoic Altaids

To-date four skarn gold deposits (Nos. 61 to 64) have been reported in Northwest China (Zhao et al., 1997; Chen et al., 1997; Chen, 2001; Li, 2002), for which no isotopic data are directly available from the skarn gold ores and their associated intrusions. However, the latter are emplaced in the Lower Carboniferous strata and probably formed in the Late Carboniferous to Permian period. The intrusions have high potassium contents and are regarded as coeval with late-orogenic shoshonite volcanic rocks (Zhang et al., 2003b). Based on 16 K–Ar ages between 280 and 240 Ma for the shoshonite rocks of the Aikendaban Formation (Chen, 2001; Bao, 2001) the skarn gold deposits most likely formed in the Permian. In a separate study, Li et al. (1998) carried out isotopic dating on most of the significant hydrothermal deposits in Northwest China. They used Sm–Nd or Rb–Sr methods on ores or fluid inclusions within mineral separates of quartz, calcite, sphalerite and pyrite formed in the metallogenic process. Their results show that most the gold–copper deposits formed in the Late Palaeozoic, whereas the gold deposits (except for epithermal and VHMS types) formed after 320 Ma (Fig. 5). The epithermal and VHMS-type deposits show Devonian–Early Carboniferous and Late Carboniferous–Permian metallogenic events for stratiform and vein-like orebodies, respectively. Chen (2000b, 2001), Chen et al. (2001, 2003) and Bao (2001) interpreted the latter event in terms of reactivation during collisional tectonism. Many authors believe that the large-scale metallogenesis in the Tian Shan–Altay Orogens occurred in the Late Carboniferous–Permian period (Chen and Zhang, 1991; Chen, 1997, 2000b, 2001; Li et al., 1998; Gu et al., 1999, 2001; Chen et al., 2000a, 2001, 2003; Rui et al., 2002; Zhang et al., 2003a). Consequently, most orogenic–mesothermal gold deposits in Northwest China, including skarn gold deposits, were formed during the Hercynian, accompanying and following destruction of oceanic lithosphere and continental collisions in the Altaid orogenic belts (Mao et al., 2003).

5.2. Southwest China: Cenozoic Tibet–Sanjiang Orogen

In the Cenozoic Tibet–Sanjiang collisional orogenic belt, the Yulong porphyry–skarn Cu–Au deposit (No. 70; Table 1), as well as the Zhalaga, Duoxiasongduo, Malasongduo porphyry–skarn gold deposits were formed. These deposits are not shown in Fig. 1 and Table 1, because most geologists consider that they are porphyry systems (e.g., Rui et al., 1984). Ore-bearing intrusions yielded thirteen K–Ar isotopic ages from 26 Ma to 64 Ma, and a Rb–Sr isochron age of 41 Ma (Rui et al., 1984). Re–Os dating on molybdenite from the Malasongduo porphyry–skarn Cu–Au deposit

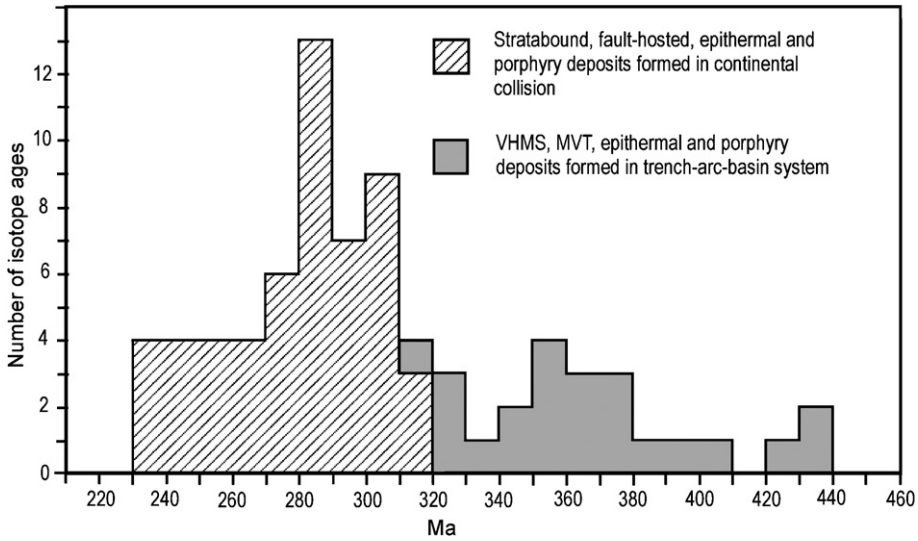

Fig. 5. Histogram of isotopic ages of hydrothermal deposits in Northwest China (data available from the senior author on request).

yielded ages of 35.4±1.3 Ma to 36.2±1.1 Ma (Tang and Luo, 1995). An isotope age histogram for the deposits and their related intrusions in the Qiangtang Block shows that the metallogenic and magmatic peak has occurred around 41 Ma (Fig. 6A). These ages are younger than the final closure of the Banggong–Nujiang Ocean (98 Ma), i.e. younger than initial collision of the Lhasa Block with the Qiangtang–Indochina Block (Fig. 4C and D). They do however track the collision of India with the Lhasa–Eurasia continent (Fig. 4E and F), in that collision began in the west between 66 and 50 Ma and progressively migrated eastward (Yin and Nie, 1996).

Recently, Rui et al. (2003) report the isotope ages for a newly discovered Gangdese porphyry–skarn Cu (Mo)–Au ore belt in the Lhasa Block (all the deposits and related intrusions are not shown because no gold reserve have been reported yet). Zircon SHRIMP ages for Qulong and Chongjiang adamellitic porphyries are 17.58±0.74 Ma and 15.60±0.52 Ma respectively,

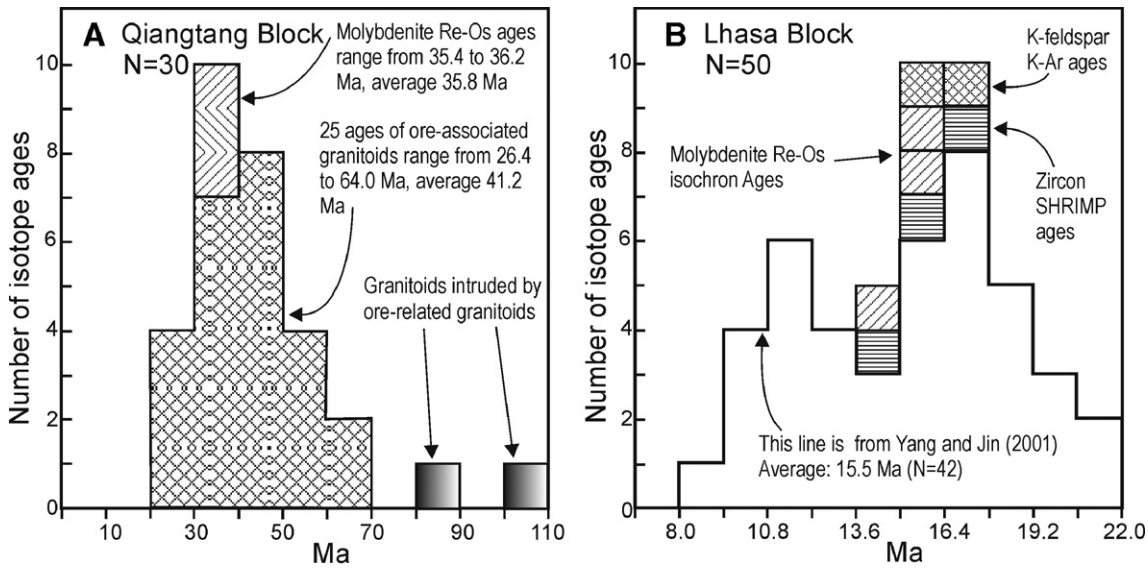

Fig. 6. Histogram of isotopic ages of granitoids and related deposits in Southwest China. (A) Histogram of isotope ages for ore-related granitoids in the Yulong metallogenic belt in the Qiangtang block (data available from the senior author on request). (B) Histogram of isotope ages for ores and related granitoids in the Lhasa Block (slightly modified after Yang and Jin, 2001).

while the Chongjiang barren diorite porphyry yields a zircon SHRIMP age of 14.54±0.65 Ma. K–Ar dating of K–feldspar from the Qulong and Chongjiang ore-associated intrusions yields ages of 16.43±0.31 Ma and 15.77±0.45 Ma, respectively. Molybdenite Re–Os isochron ages of the Qulong and Chongjiang Cu–Au deposits are 15.99±0.32 Ma and 14.85±0.69 Ma, respectively (Rui et al., 2003), and a molybdenite Re–Os isochron age of the Bangbu porphyry-type Cu–Mo–Pb–Zn deposit in the Gangdese metallogenic belt is 15.32±0.79 Ma (Meng et al., 2003). All these ages are in the time span of 8 to 22 Ma estimated for granitoids in the area (Fig. 6B), suggesting that the large-scale metallogenesis and granitic magmatism postdated the final closure of the Indus–Yalong Ocean (Fig. 4E, and F) by about 50 Ma.

5.3. East China: Mesozoic orogenic areas

Hu (1991) pointed out that economic skarn deposits in East China mostly formed in the Mesozoic and that isotopic ages of the skarn deposits and related intrusions peaked at 140–130 Ma, at the Jurassic–Cretaceous transition. This is substantiated by the isotope age data for granitoid intrusions and volcanic rocks related to hydrothermal mineralisation in East China (Fig. 7). It is further supported by the skarn gold deposits and their associated intrusions being emplaced in the Middle and Late Jurassic and Early Cretaceous (Table 2). Thus, granitoids of the Shuikoushan orefield (Nos. 9 and 10) give K–Ar and Rb–Sr isochron ages of 149 to 106 Ma (Chen and Zhu, 1993) and zircon U–Pb age of ca 172 Ma (Zhang et al., 2007-this volume-b). The Lower Yangtze River region has 124 isotopic ages of skarn gold related intrusions and volcanic rocks ranging from 180 to 60 Ma (data in Hu et al., 1991, and therein), with 91 of them concentrating between 140 and 90 Ma; Pan and Dong (1999) took 120 Ma as the peak time for the formation of skarn gold associated intrusions in this area. In the Tan-Lu fault-controlled magmatic belt, the intrusions related to the Jinchang skarn gold deposit (No. 48) are dated at 126.6 Ma by the Rb–Sr isochron method (Zhao et al., 1992), while 116 isotopic ages from the Taihang fault-controlled magmatic belt (Fig. 1)

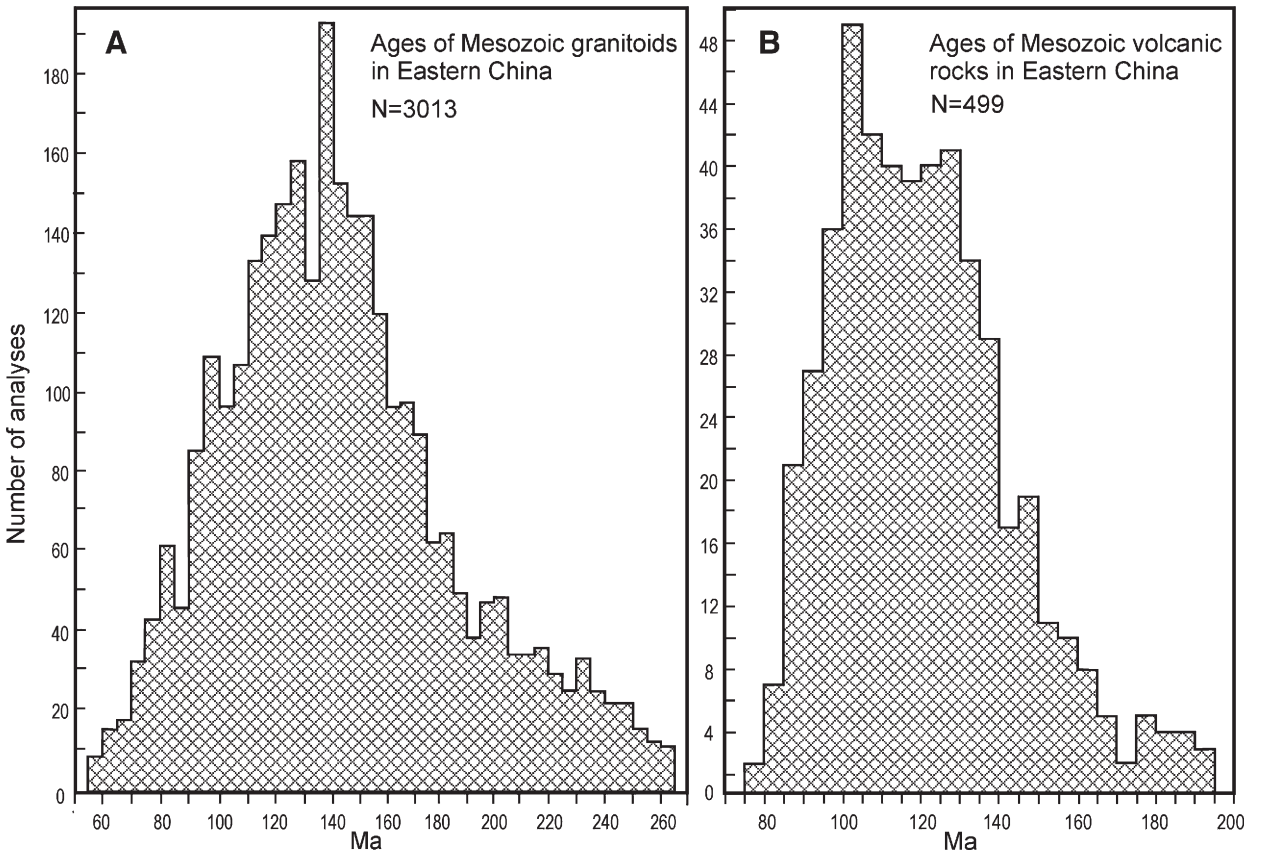

Fig. 7. Histogram of isotopic ages of ore-related granitoids in East China (A, from Hu et al., 1997) and volcanics (B, from Wang et al., 1998).

Table 2
Isotopic ages for various metallogenic Provinces and typical skarn gold deposits in China

Metallogenic province	Age range of ore and metallogenic intrusion (number)	Peak age (number)	Age of typical skarn gold deposit	Data source
East China	70–250 Ma (611)	130±10 Ma (200)		This paper
Hingan Mountains (Northeast China)	90–220 Ma (225)	120–140 Ma (85)	Laozuoshan: 123~146 Ma (K–Ar) for porphyry	Zhou et al., 2002b; this paper
Yan Shan (northern margin of North China Craton)	100–195 Ma (28)	100–145 Ma (22)	Shouwangfen: 148±4 Ma (Re–Os) for molybdenite; 130 Ma (Rb–Sr) and 127 Ma (K–Ar) for granodiorite	Zhang and Sun, 1988; Rui et al., 1994; Huang et al., 1996
Taihang fault belt	97–187 Ma (116)	102~140 Ma (57)	Diaoquan: 128 Ma (K–Ar) for biotite of ore-associated intrusion	Chang, 1997
Tan-Lu fault belt	90–170 Ma (169)	135–100 Ma (140)	Jinchang: 126.6±0.3 Ma, 154.8±0.3 Ma (Rb–Sr) and 121.6 Ma (K–Ar) for intrusions	Zhao et al., 1992; Wang et al., 1998
East Qinling–Dabie Shan	80–190 Ma (76)	120–140 Ma (31)	Yinjiagou: 152 Ma (Rb–Sr) for ore-associated granitic porphyry	Hu and Guo, 1978; this paper
Lower Yangtze River region	60–180 Ma (124)	90–140 Ma (91)	Shizishan: 138.0±2.5 Ma (Os/Os), 139.02±0.34 Ma (Re–Os)	Hu et al., 1991; Sun et al., 2003
Huanan orogen	80–200 Ma (114)	110–160 Ma (73)	Shuikoushan Orefield (Nos. 9, 10): 127.6 Ma (Rb–Sr) for ore-associated intrusion, 172 Ma (zircon U–Pb) for granodiorite	Chen and Zhu, 1993; Zhang et al., 2006-this volume-b; this paper
Southern margin of Yangtze Craton	90~160 Ma (21)	125 Ma	Dulong: 95~118 Ma (K–Ar) for intrusions	Song, 1994; this paper;
West China				
Tian Shan–Altay	230–320 Ma (46)	280–290 Ma (13)	Ashale: 280 Ma (K–Ar)	Chen, 2001
Western Central China Orogen	100–220 Ma (62)	160–180 Ma (22)	Deerni: 180–197 Ma (K–Ar) for intrusion	Duan, 1998; Chen et al., 2004a,b
Qiangtang Block (Yulong belt)	26–64 Ma (30)	Average: 41 Ma	Yulong–Malasongduo: 35.4±1.3~36.2±1.1 Ma (Re–Os) for molybdenite of ores	Tang and Luo, 1995; this paper
Lhasa Block	8–22 Ma (42)	Average: 15.5 Ma		Yang and Jin, 2001

range from 186.9 to 87 Ma, with 57 of them in the period of 140 to 102 Ma (Chang, 1997). A granodiorite associated with the Shouwangfen skarn-type Cu–Au deposit (No. 56; Table 1) in the Yan Shan area yields Rb–Sr isochron age of 130 Ma (Zhang and Sun, 1988) and K–Ar age of 127 Ma (Rui et al., 1994), while molybdenite yields a Re–Os isochron age of 148±4 Ma (Huang et al., 1996). Finally, the porphyry intrusion associated with the Laozuoshan gold deposit (No. 58; Table 1) in Northeast China (Hingan Orogen) is dated at 123 to 146 Ma by K–Ar method (Zhou et al., 2002b).

Fig. 8 is a summary of isotope ages of ores (including skarn gold) and/or ore-associated intrusions in East China and shows that most age data concentrate at ca. 130 Ma, postdating the Dongnanya–Eurasia collision (Fig. 4C) by about 50 Ma.

5.4. Central China Orogen: Mesozoic collision orogen

In the Central China Orogen (Fig. 1), oceanic closure terminated in the Late Triassic, but crustal shortening, thickening and deformation continued into the Early and Middle Jurassic (Hu et al., 1988; Chen, 1990, 1998a,b; Yin and Nie, 1996; Yuan, 1996; Zhu et al., 1998) This is supported by the development of extensional basins (Chen, 1990; Chen and Fu, 1992), paleomagnetic (Zhu et al., 1998), and seismic

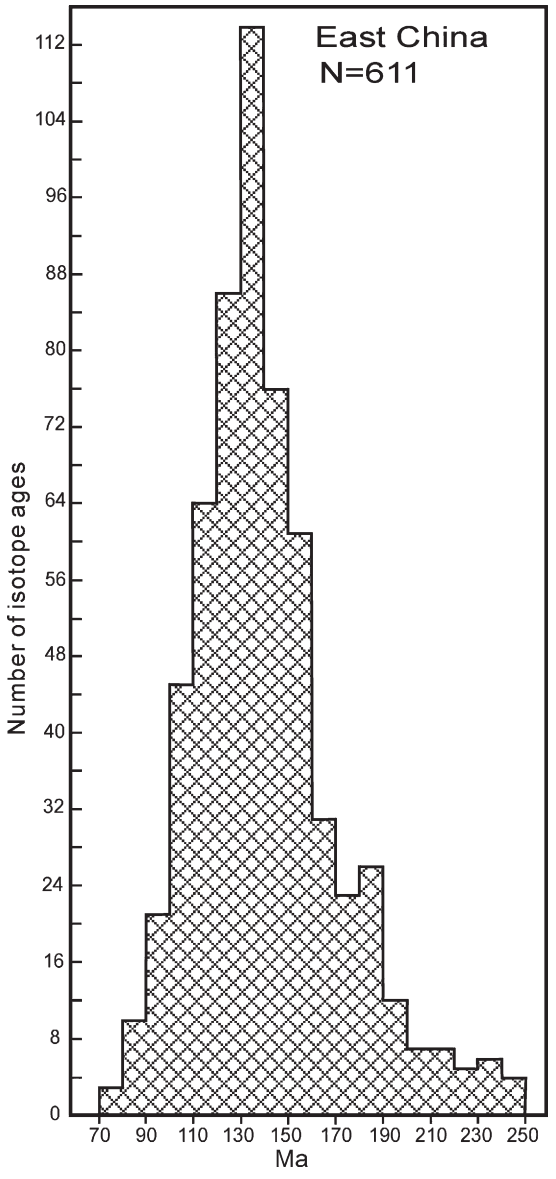

Fig. 8. Histogram of isotopic ages of ores and ore-associated intrusions (data available from the senior author on request).

reflection data (Yuan, 1996), the age of the foreland fold-and-thrust belt, and development of collisional S-type granitoids from 220 Ma (Sun et al., 2002). In the East Qinling–Dabie Shan area, 204 isotopic ages of granites related to hydrothermal deposits including porphyry/skarn systems range from 240 to 80 Ma, with most being around 130 Ma (Fig. 9A) (Hu et al., 1988, 1997; Chen and Fu, 1992; Stein et al., 1997; Huang, 1998; Li et al., 2001); while 76 isotope ages of ores, ore-hosting altered rocks and ore-associated intrusions range from 190 to 80 Ma, and peak at 130 Ma (Fig. 9B, Table 2). The Rb–Sr isochron age of the porphyry associated with the Yinjiagou deposit (No. 51) is 152 Ma (Hu and Guo, 1978).

Metallogenesis in the western parts of the Central China Orogen (West Qinling–Kunlun orogenic belts) occurred earlier than in the eastern portion, despite the fact that oceanic closure is younging westward (Chen, 2002). Mao et al. (2002) argue that large-scale metallogenesis occurred over the period from 250 to 180 Ma. However, based on all the isotope data and many deposits being hosted in Triassic strata, we contend that the metallogenic peak occurred around 170 Ma (Fig. 10; Table 2). The Baxi gold deposit (No. 65) is hosted in Triassic strata and should have formed after 208 Ma (Triassic–Jurassic boundary age). A granite intrusion associated with the Deerni deposit (No. 66) yields K–Ar ages of 180–197 Ma (Duan, 1998). The skarn gold deposits in the western Central China Orogen are therefore interpreted as Yanshanian (Chen et al., 1997, 2004b; Zhao et al., 1997; Mao et al., 2002), although we acknowledge that the current dearth of geochronological data precludes a more precise assessment of the timing of skarn gold metallogenesis.

6. Geodynamic settings of skarn gold deposits in China

6.1. Preamble

The principal geodynamic model for the origin of porphyry copper deposits in the Pacific Rim (Sillitoe, 1972) led most geologists to relate skarn deposits and their associated magmatism to oceanic plate subduction (Hu and Guo, 1978; Rui et al., 1984; Sillitoe, 1989, 2002; Quan et al., 1992; Zhao et al., 1997, 1999; Pirajno and Bagas, 2002). However, the available geochronological data and geological observations indicate that metallogenesis in the orogenic belts of Northwest China, Southwest China, East China and Central China, postdated local oceanic closure. In East China (apart from northeasternmost China), the metallogenic provinces are far from any hypothetical Mesozoic subduction zone east of the island of Taiwan and the Japanese archipelago (Fig. 4D, E and F), and their trends are usually perpendicular to, rather than parallel, to the subduction zone (e.g., Lower Yangtze River District, Central China Orogen and Yan Shan, Figs. 1 and 3). These features are inconsistent with the notion that only subduction of oceanic plates can generate the felsic magmatism that is commonly associated with skarn gold deposits. We propose, on the basis of age data and geological observations presented above, that the

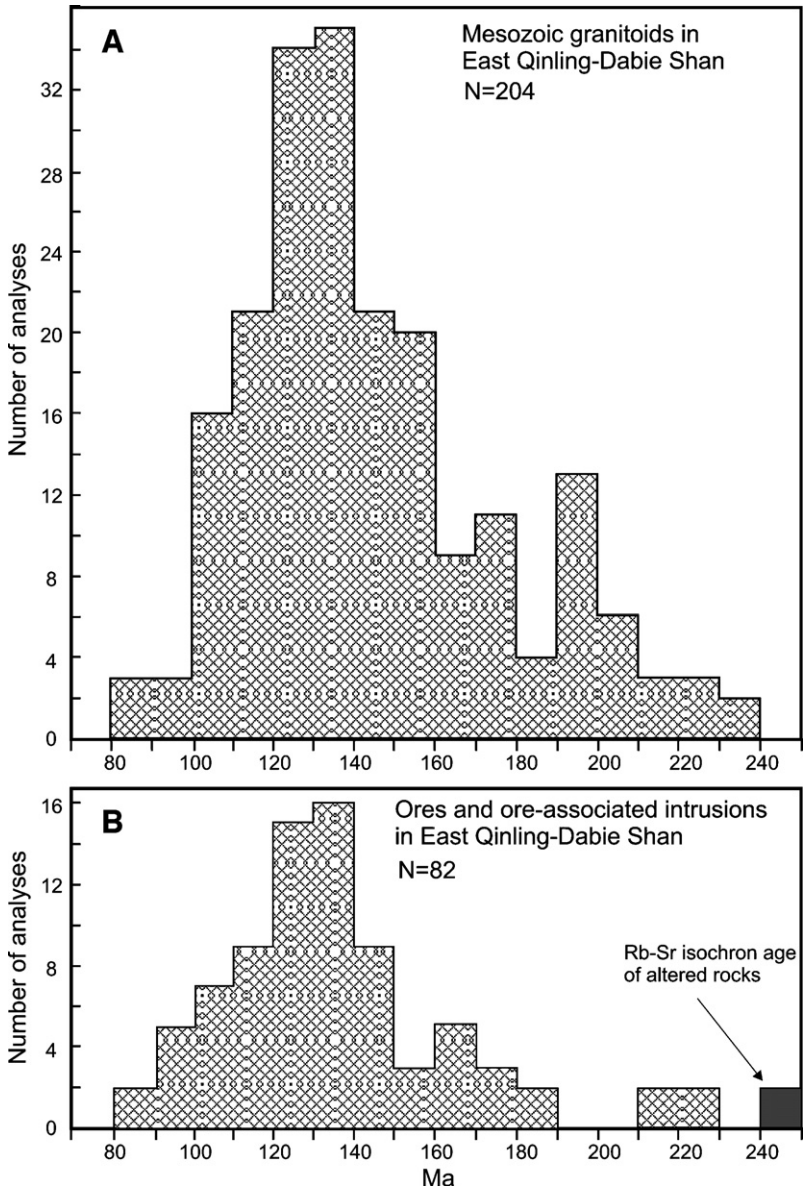

Fig. 9. Histogram of isotopic ages of granitoids (A, from Li et al., 2001) and ores and ore-associated intrusions (B, data available from the senior author on request) in the eastern portion of the Central China Orogen (East Qinling–Dabie Shan).

space–time relationship of the skarn gold deposits in China are in fact more consistent with the geodynamics of continental collisions.

A holistic view of the geodynamics of a collision event must include the early shortening, the shortening–extension transition and the late extension stages, with the P_{max} and T_{max} as dividing criteria (Fig. 11). The transition stage accommodates decompression and increasing geothermal gradients, thereby resulting in granitic magmatism, fluid generation and migration, phase separation and mixing (e.g., meteoric and deeply sourced fluids), as well as fluid–rock interaction (Chen, 1998a,b). This geodynamic regime favours development of volcanic rocks of shoshonitic affinity and of the emplacement of K-rich and K-feldspar porphyritic granitoids (KCG; Barbarin, 1999) that may be associated with peraluminous and/or followed by A-type granitoids, respectively (Chen and Fu, 1992; Chen, 1997; Wang et al., 1998; Chen et al., 2000b; Bao, 2001; Zhang et al., 2002, 2003b). Shoshonitic volcanic rocks and sub-volcanic KCG intrusions are especially favourable for the genesis of intrusion-related gold/copper

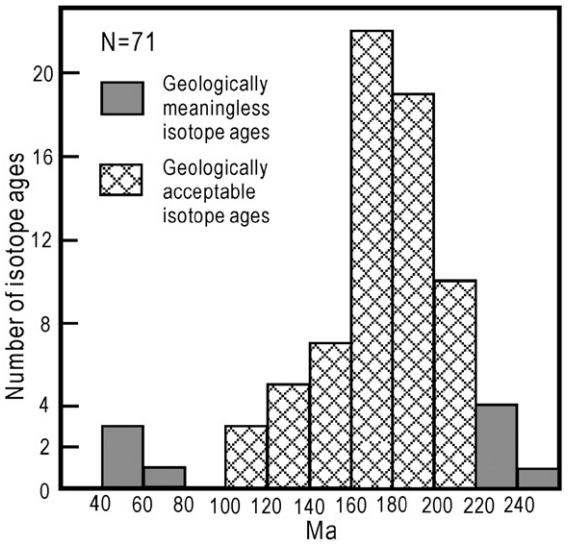

Fig. 10. Histogram of isotopic ages of gold deposits in the western portion of the Central China Orogen (Kunlun–West Qinling Mountains) (from Chen et al., 2004b).

deposits (e.g., Sawkins, 1984; Hu et al., 1988; Wang et al., 1998; Pan and Dong, 1999; Zhao et al., 1999; Lang and Baker, 2001; Sillitoe, 2002; Muller, 2002).

6.2. Geodynamic setting of skarn metallogenesis in West China

In Northwest China, the Paleoasian Ocean closed at the end of the Early Carboniferous (>322.8 Ma), and was followed by collision between the Siberia (or Angara Craton) and Tarim–North China Plates (Figs. 1–3). This suggests that the peak–metallogenesis and granitic magmatism occurred at around 285 Ma (Fig. 5; Tables 2 and 3) during continental collision, and the collision resulted in crustal thickening, shortening and uplift of the Altaids, as indicated by the lack of Late Carboniferous strata, wide development of Late Carboniferous–Early Permian peraluminous granite (Zhang et al., 2003b) and intense imbricate thrusting at various scales, as revealed by geological and geophysical data (Chen, 2000b and therein). According to Gu et al. (1999), Jahn et al. (2000) and Zhang et al. (2003b), peraluminous granites are

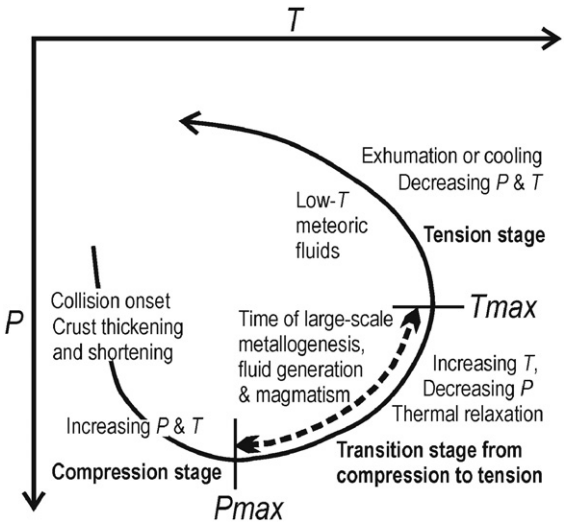

Fig. 11. *P–T–t* path for collisional Orogens (adapted from Chen, 1998b).

Table 3
Temporal relationships of oceanic closure and large-scale metallogenesis

Metallogenic Province	Youngest ocean or suture	Final ocean closure and reference	Metallogenic peak time	Time interval
East China				
Hingan and Yan Shan	Solonker	242 Ma; Robinson et al., 1999	130 Ma	112 Ma
Hingan and Yan Shan	Mongol–Okhotsk	60 Ma; Sengor and Natal'in, 1996	130 Ma	−70 Ma
Hingan and Yan Shan	Amur	>135 Ma; Sengor and Natal'in, 1996	130 Ma	>15 Ma
Taihang and Tan-Lu	Mian–Lue	T3 (220 Ma); Sun et al., 2002	130 Ma	83 Ma
East Qinling–Dabie	Mian–Lue	T3 (220 Ma); Sun et al., 2002	130 Ma	83 Ma
Lower Yangtze River Region	Xiangganzhe	T2 (230 Ma); Hsu et al., 1988	130 Ma	100 Ma
South margin of Yangtze Craton	Jinshajiang–Red River	>208 Ma; Yin and Nie, 1996	130 Ma	>78 Ma
Huanan Orogen	Gunanhai	J1 (180 Ma); Hsu et al., 1988	130 Ma	50 Ma
In general	Gunanhai	180 Ma	130 Ma	50 Ma
West China				
Tian Shan–Altay	Kalamaili–dalabute	>=322.8 Ma; Chen, 1997	285 Ma	>38 Ma
Kunlun–West Qinling	Mian–Lue	T3 (220 Ma); Sun et al., 2002	170 Ma	50 Ma
Qiangtang Block	Bangong–Nujiang	≅98 Ma; Yin and Nie, 1996	41 Ma	57 Ma
Lhasa Block	Indus–Yalong	66–50 Ma; Yin and Nie, 1996	<16 Ma	≈50 Ma

Peak–metallogenic times are discussed in text.

intruded by K-rich granites, with ages clustering between 300 and 260 Ma, followed by A-type granites of <260 Ma. The K-rich granitoids and A-type granitoids are coeval with shoshonitic rocks such as the Aikendaban Formation (Bao, 2001; Chen, 2001). These K-rich granitoids and shoshonitic volcanic rocks were probably developed in a regime of decompression and increasing geothermal gradient; with the A-type granites probably marking the end of collision, because they are overlain by Late Permian basalts and coal-bearing strata (Bao, 2001; Zhang et al., 2003b). Hence, the magmatism and associated skarn gold deposits in Northwest China most probably formed in a regime of decompression and increasing geothermal gradient, during the transition from collisional shortening to extension, approximately >38 Ma after the final oceanic closure (Table 3).

In the western portion of the Central China Orogen (Kunlun–West Qinling orogenic belts), the Baxi deposit (No. 65; Table 1) is hosted in Triassic strata deposited in a foreland basin (Table 1), on south side of the north-dipping Maqu–Mian–Lue Fault (Fig. 1) interpreted as the suture derived from an oceanic closure (Fig. 4B). This setting rules out the possibility of relating the Baxi deposit and associated intrusion to north-directed oceanic subduction. The other four deposits (Nos. 66 to 69; Table 1) are hosted in deformed Palaeozoic–Triassic strata and therefore should have formed after Triassic oceanic closure. Granitoids and the associated large-scale metallogenesis (particularly, the Carlin-type and Carlin-like gold deposits) in the area occurred around 170 Ma (Tables 2 and 3) (Chen et al., 2004b). Thus, granitic magmatism and related peak–metallogenesis postdated oceanic closure (ca. 220 Ma) by 50 Ma.

Age data for the Yulong Cu–Mo–Au deposit (No. 70) prove that granitic magmatism and metallogenesis postdated the onset of the collision between the Lhasa and Qiangtang–Indochina blocks (Fig. 4C and D) by ca. 57 Ma (Table 3). Here too magmatism is K-rich and includes rocks of shoshonitic affinity (Rui et al., 1984). The shortening-to-extension transition and the dextral strike–slip along the Jinshajiang–Red River fault systems (Fig. 4E and F) (Yin and Nie, 1996; Harrison et al., 1996) may have facilitated development of these shoshonitic intrusions.

The India–Eurasia collision (Fig. 4E and F) began between 66 and 50 Ma (Yin and Nie, 1996). Immediately south of the Indus–Yalong suture (Himalaya Orogen), there are peraluminous leucogranites and coeval tin deposits, yielding isotopic ages ranging from 22 to 8 Ma and concentrating at 15.5 Ma (Yang and Jin, 2001), while porphyries and associated Cu–Au deposits of the Gangdese metallogenic belt are present north of the suture (the Lhasa Block in Fig. 1) and yield isotope ages ranging 17.58–14.85 Ma (Rui et al., 2003). These granitoids indicate a compressional tectonic setting and can be regarded as the precursor to KCG and shoshonitic magmatism. This means that, since 22 Ma, the Gangdese–Himalaya Mountains has probably entered into a stage of collisional shortening-to-extension transition.

In summary, although the closure of paleo-oceans in West China occurred at different times and tend to young southward, large-scale granitic magmatism and related metallogenesis in various tectonic units always took place during a regime of collisional shortening-to-extension transition, and postdated the local final oceanic closure by about 50 Ma (Table 3).

6.3. A uniform geodynamic setting of coeval metallogenesis in East China

As the southeastern portion of Eurasia continent, East China was affected by the Eurasia–Pacific interaction. This has led most geologists (e.g. Rui et al., 1984; Quan et al., 1992; Zhao et al., 1997, 1999) to consider that East China belongs to the huge circum-Pacific metallogenic belt, and consequently to relate the Mesozoic magmatism and metallogenesis in East China to the northwestward subduction of the Pacific plate beneath the Eurasia plate. We suggest that this relationship is not consistent with observations discussed in this paper and summarised below: (1) large-scale metallogenesis and granitic magmatism in East China occurred during the Yanshanian and peaked around 130 Ma (Tables 2 and 3), contrasting in time with the Cenozoic metallogenesis that took place in other areas (e.g., Japan, Taiwan and other islands in western Pacific Ocean, and the Andean belt in western South America); (2) important metallogenic provinces, such as the Yan Shan, Lower Yangtze River region and Southern China metallogenic provinces (Figs. 1 and 3), East Qinling (Mo, Au, Ag) (Hu et al., 1988; Chen et al., 2000b) and Jiaodong (Au) (Chen et al., 2004a), all trend perpendicular, and not parallel to the Mesozoic and present-day trenches (Fig. 3; Sengor and Natal'in, 1996); (3) these metallogenic provinces are 500–2000 km far from any hypothetical Mesozoic subduction zone (for detail, see Sengor and Natal'in, 1996) that is postulated east of the island of Taiwan and the Japanese archipelago, thereby ruling out the possibility that magmatism and related metallogenesis occurred in a subduction-related magmatic arc system; and (4) granitoids in most metallogenic provinces are dominated by S-type, and not I-type typical of subduction-related magmatic arc systems.

All of these features suggest that the Yanshanian granitic magmatism and related metallogenesis in East China probably occurred in a geodynamic regime of continental collisions.

The difference in the timing of metallogenic events, between the eastern and western parts of the Central China Orogen, provides important clues in the understanding of the tectonic setting for large-scale Yanshanian metallogenesis in East China. Taking the 108°E meridian line as an arbitrary boundary, granitoids and the related large-scale metallogenesis in the eastern part of the Central China Orogen occurred around 130 Ma, and lagged behind that in the west (ca. 170 Ma) by 40 Ma (Tables 2 and 3, above). The Yinjiagou skarn deposit (No. 51) and the coeval Jinduicheng–Luanchuan porphyry–skarn Mo–W–Au belt (Chen et al., 2000b) formed in the shortening-to-extension transition regime (Chen and Fu, 1992; Chen et al., 2000b). The host rocks are KCG intrusions (Chen et al., 2000b) that occasionally coexist with Early Cretaceous shoshonitic volcanic rocks (HBGMR, 1989b). Considering that the peak–metallogenesis around 170 Ma in the western parts of the Central China Orogen also occurred in a shortening-to-extension transition regime, we postulate that a shortening-to-extension transition event in the eastern part of the Central China Orogen occurred around 130 Ma, and not at around 170 Ma. This event must be the Early Jurassic Dongnanya–Eurasia collision (Fig. 4C), which affected East China in the Jurassic.

The continental collisions in East China began in Permo-Triassic times along the Solonker suture (Fig. 3), followed by Triassic multi-continental collisions to the south (Fig. 4A and B), and the Early Jurassic Dongnanya–Eurasia collision (Fig. 4B and C). During this sequence of collisional events, the whole of East China was subjected to strong compression, which resulted in the development of peraluminous granites. In the subsequent period from 180 Ma to 98 Ma, no significant collisions occurred and the geodynamic conditions involved a change from shortening to extension (Figs. 4C–E and 12). Moreover, the northward subduction of the Bangong–Nujiang Ocean, the southward subduction of the Mongol–Okhotsk Ocean and the westward subduction of the Pacific Ocean could have concurrently caused back-arc extension (Fig. 12). It is therefore not surprising that large-scale granitic magmatism (especially KCG and shoshonitic rocks), fluid generation and hydrothermal metallogenesis, including skarn-type mineralisation, occurred between 180 and 98 Ma, and peaked around 130 Ma. Peak metallogenesis in East China, including the eastern part of Central China Orogen, postdated the final closure of the Gunanhai Ocean by about 50 Ma, as is also the case in West China and other collisional orogens worldwide (Kerrich et al., 2000; Goldfarb et al., 2001).

7. Tectonic model of skarn gold deposits in China

Sillitoe (1972) linked the genesis of porphyry copper deposits of the circum-Pacific region to subduction tectonics and many authors (e.g., Rui et al., 1984, 1994; Wu, 1990, 1992, 1994; Zhao et al., 1990, 1992, 1997, 1999; Chang et al., 1991) attempted to explain the formation of skarn deposits in China, using Sillitoe's model, mainly because mainland China

is adjacent to the Pacific Ocean. However, the timing of the ore-forming processes, spatial distribution and geodynamic setting of skarn gold deposits in China are inconsistent with this model, and compel us to offer an alternative view, namely that most gold skarn deposits in China formed under the collision geodynamics involving a transitional regime from shortening to extension.

7.1. Features of a collisional orogen and the foundations of a metallogenic model

At present, there is a general agreement on two aspects of the geology of collisional orogens. One is the *P–T–t* path (Fig. 11), which outlines the physical parameters and temporal evolution of the geodynamics of a collisional event (e.g., Jamieson, 1991). The other is

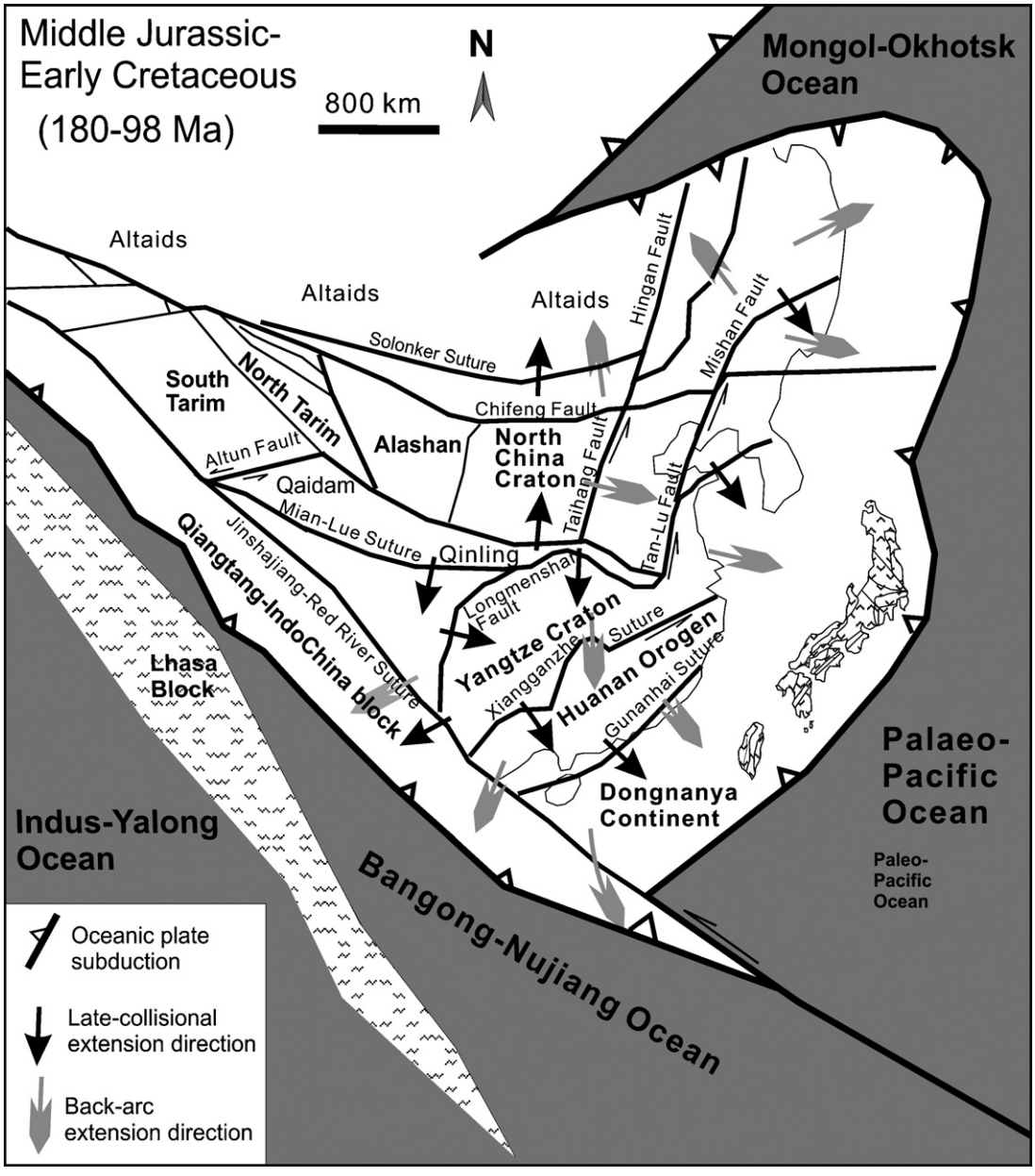

Fig. 12. Geodynamic setting for large-scale metallogenesis and granitic magmatism in East China (compiled mainly according to Hsu et al., 1988; Sengor and Natal'in, 1996; Yin and Nie, 1996).

the structural geometry (Fig. 13A) involving the stacking of thrusts and thin-skinned tectonics, as in A-type/intracontinental subduction (e.g., Bird, 1978; Hsu, 1979; Sengor, 1990).

The cause of the geothermal gradient increase from P_{max} to T_{max} in the P–T–t path (Fig. 11) has been poorly interpreted to date. We ascribe it to four processes: (1) transformation of stress energy into heat energy; (2) accumulation of radioactive elements as a result of crustal thickening, principally because K, U, Rb and Th tend to be concentrated in the upper crust; (3) upward movement of material from the asthenosphere during mantle–crust interaction, such as lithospheric delamination and mafic magma underplating; and (4) heat-release from metamorphic reactions such as the formation of UHP rocks.

7.2. Elements of the CMF model

Based on work conducted in the Qinling Orogen, Chen (1990, 1997, 1998a,b) proposed a holistic model that links collisional orogeny, petrogenesis, metallogenesis, fluid generation and fluid flow (abbreviated to CMF) as a consequence of collision tectonics. The CMF model, schematically illustrated in Fig. 13, comprises three principal elements: (1) underthrusting or A-type subduction systems, which tend to develop a spatial zonation from orogenic-type hydrothemal deposits (zone D), to deposits associated with batholithic granitoids (zone G) and porphyry intrusions (zone P) in the hangingwall slab, due to the P–T-increase of the underthrust slab; (2) petrogenesis (including metamorphism and magmatism), fluid generation and fluid flow, and metallogenesis, which reflect three stages in their evolution, namely early shortening, the shortening–extension transition, and late extension; and (3) large-scale petrogenesis (magma generation), fluid generation and metallogenesis mainly occur during the shortening–extension transition regime, due to decompression, increasing geothermal gradient, and the geothermal fluctuations that result from imbricate thrusting.

The CMF model enables the metallogenesis of most collisional orogens to be well understood, because this model envisages batholithic granitoids, porphyry intrusions and hydrothermal ore deposits as the combined effects of the interaction between two colliding continents/terranes, with a spatial and temporal coherence with regard to various types of ore deposits. For example, orogenic-type gold and silver deposits, skarn-type, porphyry-type and Carlin-type, together with porphyry–skarn Mo–W deposits, low-temperature hydrothermal Hg–Sb deposits, were concurrently formed in the Qinling orogenic belt (Chen and Fu, 1992; Chen et al., 2000b, 2004b).

8. Skarn gold deposits in China and the CMF model: discussion and conclusion

We suggest that the genesis of most skarn gold deposits in China can be explained by the CMF model, as illustrated in Fig. 13.

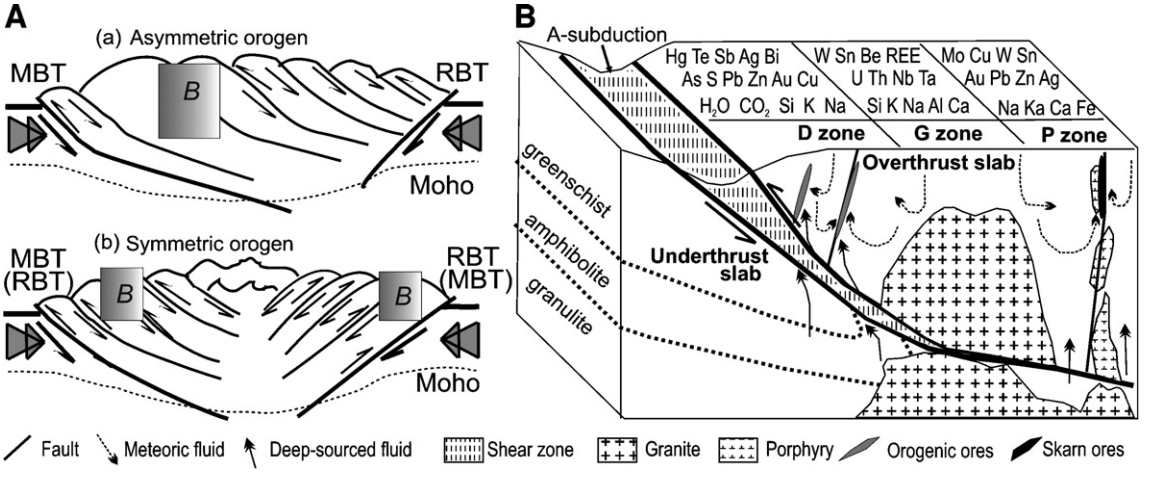

Fig. 13. Tectonic model for skarn gold deposits and their hosting intrusions in China. (A) Structural geometry of a collisional orogen (adapted from Sengor, 1990), MBT and RBT denote the main and reverse boundary thrust faults. (B) Tectonic model for collisional petrogenesis, fluid generation and metallogenesis (from Chen, 1990, 1998b): D, orogenic–mesothermal deposits zone; G, granite batholith and associated deposits zone; P, porphyry and associated deposits (including skarn gold) zone.

The skarn gold deposits in China are located in the collisional orogenic belts, intracontinental fault-controlled magmatic belts and reactivated/rejuvenated cratonic margins. Igneous activity in the intracontinental fault-controlled magmatic belts and reactivated cratonic margins is contemporaneous with that in the collisional orogens. Some additional explanation is needed for skarn gold deposits along the Tan-Lu and Taihang fault-controlled magmatic belts, since these are discordant to the dominant orogenic trends. During the Triassic–Early Jurassic N–S collision, these two major fault zones were accommodated by strike–slip motion and E–W extension (possibly as pull-apart). In addition, during the decompression–extension stage that affected East China, these fault zones again acted as extensional structures (Chen et al., 1998). In such conditions, the fault zones would be loci of decompression and higher geothermal gradients, thereby resulting in more intense development of magmas of shoshonitic affinity, which are conducive to and associated with gold-bearing skarn- and/or porphyry-types mineralisation. According to the CMF model, a zonation of mineral deposit types would be expected along the two fault belts, but this is not observed, probably because the attitude of the fault zones is nearly vertical.

The skarn gold provinces of China occupy four tectonic domains: (1) the western portion of the Chinese Altaids in Northwest China; (2) the western portion of the Central China Orogen including Kunlun/Qilian–West Qinling orogenic belts; (3) the Cenozoic Tethysides of the Tibet–Sanjiang Orogen in Southwest China; and (4) the largest Mesozoic orogenic areas in East China, including the eastern portion of Altaids and Manchurides, the eastern portion of Central China and Huanan Orogens, as well as the Yangtze and North China Cratons (Figs. 1 and 3).

In each tectonic domain, peak-formation of the skarn gold deposits and their associated intrusions (usually KCG or shoshonitic rocks) postdated final oceanic closure by about 50 Ma. In Northwest China, the Palaeoasian Ocean closed in the Early Carboniferous (>322.8 Ma) and large-scale metallogenesis occurred around 285 Ma. In Southwest China, the Lhasa block collided with the Eurasian Plate at about 98 Ma, and the Yulong porphyry–skarn copper–gold belt developed at about 40 Ma; in the western Central China Orogen, the Kunlun–South Qinling Ocean closed at about 220 Ma and peak–metallogenesis occurred around 170 Ma. Finally, in East China, where peak–metallogenesis occurred around 130 Ma, ocean–closure eventually ended in the Early Jurassic (180 Ma) along the Guananhai suture.

The timing of these metallogenic events precludes using oceanic plate subduction in order to explain the formation and distribution of skarn gold deposits and their related intrusions. On the other hand, a spatial and temporal relationship with continental collisions strongly suggests that skarn gold deposits and their associated intrusions are genetically related to such collisions. A schematic P–T–t path for collisional orogenesis shows that the shortening-to-extension transitional regime, characterized by conditions of decompression and geothermal fluctuations with an overall trend of increasing geothermal gradient, particularly favors large-scale granitic magmatism, fluid generation and metallogenesis. Thin-skinned tectonics or imbricate thrusting/A-type subduction is characteristic of collisional orogens and leads to crustal shortening and thickening, as well as uplift and mountain building. It provides the framework for syn-collisional petrogenesis, fluid generation, fluid flow and metallogenesis (CMF model; Fig. 13).

Acknowledgments

This study was granted by the National Natural Science Foundation of China (Nos. 40425006, 40352003, 49972035 and 49672119), Institute of Geochemistry of Chinese Academy of Sciences (Hundred Young Scientists Program), Ministry of Science and Technology of China (No. 96-915-03-05) and the Education Ministry of China (key research program and trans-century teachers program). Drs. Ji Hongbing and Pan Tong provided their research results of the Baxi and Kentekeke gold deposits, respectively. Profs. L. Meinert, H. Shimazaki, Dr. T.H. Zhou, Profs. R. Newberry and D. Rickard carefully revised the earliest version of the manuscript. Professors Brian Marshall and David Lentz are thanked for their relevant comments, constructive suggestions and careful corrections on the submitted manuscript. Franco Pirajno publishes with the permission of the Director of the Geological Survey of Western Australia.

References

Allen, M.B., Windley, B.F., Zhang, C., 1992. Palaeozoic collisional tectonics and magmatism of the Chinese Tian Shan, central Asia. Tectonophysics 220, 89–115.

Allen, M.B., Windley, B.F., Zhang, C., Guo, J., 1993. Evolution of the Turpan basin, Chinese Central Asia. Tectonics 12, 889–896.

Allen, M.B., Sengor, A.M.C., Natal'in, B.A., 1995. Junggar, Turpan and Alakol basins as Late Permian to Early Triassic extensional structures in a sinistral shear zone in the Altaid orogenic collage,

central Asia. Journal of the Geological Society (London) 152, 327–338.
Bache, J.J., 1987. World Gold Deposits: A Geological Classification. North Oxford Academic, London. 179 pp.
Bao, J.X., 2001. Metallogenesis of epithermal gold–copper deposits in western Tian Shan. PhD thesis, Peking University, Beijing, China. 149 pp. (in Chinese with English abstract).
Barbarin, B., 1999. A review of the relationships between granitoid types, their origins and their geodynamic environments. Lithos 46, 605–626.
Beddoe-Stephens, B., Shepherd, T.J., Bowles, J.F.W., Brook, M., 1987. Gold mineralization and skarn development near Muara Sipongi, West Sumatra, Indonesia. Economic Geology 82, 1732–1749.
Bird, P., 1978. Initiation of intracontinental subduction in the Himalaya. Journal of Geophysical Research 83, 4975–4987.
Boyle, R.W., 1979. The Geochemistry of Gold and Its Deposits. Bulletin-Geological Survey of Canada 280 (584 pp.).
Cameron, D.E., Garmoe, W.J., 1987. Geology of skarn and high-grade gold in the Carr Fork Mine, Utah. Economic Geology 82, 1319–1333.
Chang, Z.S., 1997. Genesis of skarns and skarn deposits in Taihang Mountains. PhD thesis, Peking University, Beijing, China. 210 pp. (in Chinese with English abstract).
Chang, Y.F., Liu, X.P., Wu, Y.C., 1991. The Copper and Iron Deposits in the Lower Yangtze River District. Geological Publishing House, Beijing. 379 pp. (in Chinese with English abstract).
Chen, Y.J., 1986. Types and examples of far-field impacts of plate convergence. In: Pan, L.Q. (Ed.), Postgradutes' Contributions to 65th Anniversary of Geology Department, Nanjing University, Nanjing, pp. 12–15 (in Chinese).
Chen, Y.J., 1990. The geologic characteristics, mineralization and exploration of the main types of gold deposits, West Henan. PhD thesis, Nanjing University, Nanjing, China. 169 pp. (in Chinese).
Chen, Y.J., 1996. Skarn gold deposits in China. Resource Geology 46, 369–376.
Chen, Y.J., 1997. Mineralization during collisional orogenesis and its control of the distribution of gold deposits in Junggar Mountains, Xinjiang, China. Acta Geologica Sinica 71, 69–79.
Chen, Y.J., 1998a. Constraints and their mechanism on the petrogenic and metallogenic model for collision orogenesis. Earth Science Frontiers 5, 109–118 (Suppl., in Chinese with English abstract).
Chen, Y.J., 1998b. Fluidization model for continental collision in special reference to study on oreforming fluid of gold deposits in the eastern Qinling Mountains, China. Progress in Natural Science 8, 385–393.
Chen, T.L., 2000a. Skarn deposits in Shandong Province. PhD thesis, Peking University, Beijing, China. 149 pp. (in Chinese with English abstract).
Chen, Y.J., 2000b. Progress in the study of Central Asia-type orogenesis–metallogenesis in Northwest China. Geological Journal of China Universities 6, 17–22 (in Chinese with English abstract).
Chen, Y.J., 2001. Copper and Gold Metallogeny in the Tianger–Baluntai Region, Western Chinese Tian Shan. Unpublished Research Report, Peking University, Beijing. 280 pp. (in Chinese).
Chen, Y.J., 2002. Several problems in study of regional metallogenesis in China: their relationship to continental collision. Earth Science Frontiers 9, 319–328 (in Chinese with English abstract).
Chen, Y.J., Chang, Z.S., 1996. Metallogenic model of skarn gold deposits, China. In: Zhang, Y.X., Cun, G., Liu, L.D. (Eds.), Gold Deposits in China: Advances and Considerations. Geological Publishing House, Beijing, pp. 57–69 (in Chinese with English Abstract).
Chen, Y.J., Fu, S.G., 1992. Gold Mineralization in West Henan, China. Seismological Press, Beijing. 234 pp. (in Chinese with English abstract).
Chen, Y.J., Guo, K.H., 1993. Geology, geochemistry and genesis of the Yinjiagou skarn type gold deposit. Mineral Deposits 12, 265–272 (in Chinese with English abstract).
Chen, Y.J., Zhang, C.N., 1991. The mineralization model for gold deposits in the western Zhunge'er area. Journal of Changchun University of Earth Sciences 21, 61–66 (in Chinese with English abstract).
Chen, Y.C., Zhu, Y.S., 1993. Metallogenic Models of Mineral Deposits, China. Geological Publishing House, Beijing. 367 pp. (in Chinese).
Chen, Y.J., Hu, S.X., Fu, C.Y., Ji, H.Z., Zhang, S.H., 1990a. Harmonious distribution of auriferous districts with khondalite series and the prediction of new auriferous districts. Gold Geology (1), 17–22 (in Chinese).
Chen, Y.J., Hu, S.X., Fu, S.G., 1990b. Evidence for the existence of the Sanmenxia–Baofeng fault and discussion on some related problems. Journal of Nanjing University, Earth Science Edition (3), 75–84 (in Chinese with English abstract).
Chen, Y.J., Fu, S.G., Lu, B., Ji, H.Z., 1992. Classification of genetic series and type of gold deposits. Advance in Earth Science 7 (3), 73–79 (in Chinese with English abstract).
Chen, Y.J., Qin, S., Li, X., 1997. Mineralization time, space, geodynamic background and metallogenic model of the skarn gold deposits, China. Universitatis Pekinensis 33, 456–466 (in Chinese with English abstract).
Chen, Y.J., Guo, G.J., Li, X., 1998. Metallogenic geodynamic background of gold deposits in granite–greenstone terrains of North China Craton. Science in China. Series D 41, 113–120.
Chen, H.Y., Bao, J.X., Zhang, Z.J., Liu, Y.L., Ni, P., Ling, H.F., 2000a. Isotope indication to source of ore materials and fluids of the Wangfeng gold deposit in Tianshan: a case study of metallogenesis during collisional orogenesis. Science in China. Series D 43, 56–166 (Suppl.).
Chen, Y.J., Li, C., Zhang, J., Li, Z., Wang, H.H., 2000b. Sr and O isotopic characteristics of porphyries in the Qinling molybdenum deposit belt and their implication to genetic mechanism and type. Science in China. Series D 43, 82–94 (Suppl.).
Chen, H.Y., Chen, Y.J., Liu, Y.L., 2001. Metallogenesis of the Ertix gold belt, Xinjiang and its relationship to Central Asia-type orogenesis. Science in China. Series D 44, 245–255.
Chen, Y.J., Pirajno, F., Chen, H.Y., Zhang, Z.J., Bao, J.X., Liu, Y. L., Huang, B.L., 2003. Tectonic model for collisional orogeny, metallogenesis and fluid flow (CMF) and its application in North Xinjiang, China. Extended Abstracts of International Field Symposium in Urumqi, Xinjiang, China, 9–21 August, pp. 2–6.
Chen, Y.J., Pirajno, F., Lai, Y., Li, C., 2004a. Metallogenic time and tectonic setting of the Jiaodong gold province, eastern China. Acta Petrologica Sinica 20, 907–922 (in Chinese with English abstract).
Chen, Y.J., Zhang, J., Zhang, F.X., Pirajno, F., Li, C., 2004b. Carlin and carlin-like gold deposits in Western Qinling Mountains and their metallogenic time, tectonic setting and model. Geological Review 50, 134–152 (in Chinese with English abstract).
Davis, G.A., Qian, X.L., Zheng, Y.D., Tong, H.M., Wang, C., Gehrels, G.E., Shafiquallah, M., Fryxell, J., 1996. Mesozoic deformation and plutonism in the Yunmeng Shan: a metamorphic core complex

north of Beijing, China. In: Yin, A., Harrison, T.M. (Eds.), The Tectonic Evolution of Asia. Cambridge University Press, Cambridge, pp. 253–280.

Duan, G.L., 1998. Geological characteristics of the Deerni copper–cobalt deposit, Qinghai. Mineral Deposits 17, 667–670 (Suppl., in Chinese with English abstract).

Editorial Board of AGST, 1988. Attention to skarn gold deposits: large skarn gold deposits are mined in Canada, Australia and USA. Abroad Geologic Science and Technology 8, 1–10 (in Chinese).

Einaudi, M.T., Burt, D.M., 1982. Introduction, terminology, classification and composition of skarn deposits. Economic Geology 77, 745–754.

Einaudi, M.T., Meinert, L.D., Newberry, R.J., 1981. Skarn deposits. Economic Geology, 75th Anniversary Volume 317–391.

Ettlinger, A.D., Meinert, L.D., Ray, G.E., 1992. Gold skarn mineralization and fluid evolution in the Nickel Plate deposit, British Columbia. Economic Geology 87, 1541–1565.

Ewers, G.R., Sun, S.S., 1989. Genesis of the Red Dome gold skarn deposit, Northeast Queensland. Economic Geology Monographs 6, 218–232.

Faure, M., Lin, W., Breton, N.L., 2001. Where is the North China–South China block boundary in the eastern China? Geology 29, 119–122.

Goldfarb, R.J., Groves, D.I., Gardoll, S., 2001. Rotund versus skinny orogens: well-nourished or malnourished gold? Geology 29, 539–542.

Gu, L.X., Hu, W.X., He, J.X., Xu, Y.T., 1993. Geology and genesis of the Upper Palaeozoic massive sulphide deposits in South China. Transactions of the Institution of Mining and Metallurgy, Section B: Applied Earth Science 83–96.

Gu, L.X., Hu, S.X., Chu, Q., Yu, C.S., 1999. Pre-collision granites and post-collision intrusive assemblage of the Kelameili–Harlik orogenic belt. Acta Geologica Sinica 73, 316–329.

Gu, L.X., Hu, W.X., He, J.X., Ni, P., Xu, K.Q., 2000. Regional variations in ore composition and fluid features of massive sulphide deposits in South China: implications for genetic modelling. Episodes 23, 110–118.

Gu, L.X., Hu, S.X., Yu, C.S., Zhao, M., 2001. Intrusive activities during compression–extension tectonic conversion in the Bogda intracontinental orogen. Acta Petrologica Sinica 17, 187–198 (in Chinese with English abstract).

Gu, L.X., Chen, P.R., Nie, P., Xu, Z.W., Xiao, X.J., 2002. Comparative research on ore-forming fluids for the main types of hydrothermal copper–gold deposits in the middle and lower reaches of the Yangtze River. Journal of Nanjing University, Natural Sciences 38, 392–407 (in Chinese with English abstract).

Gu, L.X., Hu, W., Khin Zaw, Nie, P., He, J., 2007. Distinctive features of Late Palaeozoic massive sulphide deposits in South China. Ore Geology Reviews 31, 107–138 (this volume). doi:10.1016/j.oregeorev.2005.01.002.

Hacker, B.R., Wang, X., Eide, E.A., Ratschbacher, L., 1996. The Qinling–Dabie ultra-high-pressure collisional orogen. In: Yin, A., Harrison, T.M. (Eds.), The Tectonic Evolution of Asia. Cambridge University Press, Cambridge, pp. 345–370.

Harrison, T.M., Leloup, P.H., Ryerson, F.J., Tapponnier, P., Lacassin, R., Chen, W.J., 1996. Diachronous initiation of transtension along the Ailao Shan–Red River shear zone, Yunnan and Vietnam. In: Yin, A., Harrison, T.M. (Eds.), The Tectonic Evolution of Asia. Cambridge University Press, Cambridge, pp. 208–226.

HBGMR (Henan Bureau of Geology and Mineral Resource), 1989a. Exploration Report of Yinjiagou Gold Deposit, Lingbao County, Henan Province. Unpublished Report, HBGMR, Luoyang, 420 pp. (in Chinese)

HBGMR (Henan Bureau of Geology and Mineral Resource), 1989b. Regional Geology of Henan Province. Geological Publishing House, Beijing. 772 pp. (in Chinese with English Abstract).

Hou, Z.Q., Khin Zaw, Pan, G.T., Xu, Q., Hu, Y.Z., Li, X.Z., 2007. Sanjiang Tethyan metallogenesis in S.W. China: tectonic setting, metallogenic epochs and deposit types. Ore Geology Reviews 31, 48–87 (this volume). doi:10.1016/j.oregeorev.2004.12.007.

Hsu, K.J., 1979. Thin-skinned plate tectonics during Neo-Alpine orogeneses. American Journal of Sciences 279, 353–366.

Hsu, K.J., 1981. Thin-skinned plate–tectonic model for collision type orogeneses. Scientia Sinica (Science in China) 24, 105–110.

Hsu, K.J., Sun, S., Chen, H.H., Pen, H.H., Sengor, A.M.C., 1988. Mesozoic overthrust tectonics in South China. Geology 16, 418–421.

Hsu, K.J., Li, J.L., Chen, H.H., Wang, Q.C., Sun, S., Sengor, A.M.C., 1990. Tectonics of South China: key to understanding of west Pacific geology. Tectonophysics 183, 9–39.

Hu, S.X. (Ed.), 1982. Mineral Deposits. Geological Publishing House, Beijing. 310 pp. (in Chinese).

Hu, S.X., 1991. Skarn deposits in eastern China. Skarns – Their Genesis and Metallogeny, Theophrastus Publications S. A. Greece, pp. 423–433.

Hu, Y.D., Guo, K.H., 1978. Structural Controlling on Mineralization in the West Henan and Prediction for Endogenic Ore Deposits. Geological Publishing House, Beijing. 133 pp. (in Chinese with English abstract).

Hu, S.X., Lin, Q.L., Chen, Z.M., Li, S.M., 1988. Geology and Metallogeny of the Collision Belt Between the North and the South China Plates. Nanjing University Press, Nanjing. 558 pp. (in Chinese).

Hu, W.X., Xu, K.Q., Hu, S.X., Ren, Q.J., 1991. Exhalative Sedimentation and Hydrothermal Transformation–Superimposition Iron and Pyrite Deposits in Ningwu–Luzong Continental Volcanic Basins. Geological Publishing House, Beijing. 142 pp. (in Chinese with English abstract).

Hu, S.X., Zhao, Y.Y., Xu, J.F., Ye, Y., 1997. Geology of Gold Deposits in North China Platform. Science Press, Beijing. 220 pp. in Chinese.

Huang, C.Q., 1978. An outline of the tectonic characteristics of China. Eclogae Geologicae Helveticae 71, 611–635.

Huang, D.H., 1998. Re–Os age and spatiotemporal relation of mineralization in main molybdenum (copper) metallogenic belts. Mineral Deposits 17, 813–816 (Suppl., in Chinese).

Huang, J.Q., Chen, B.W., 1987. The Evolution of the Tethys in China and Adjacent Regions. Geological Publishing House, Beijing. 109 pp. (English–Chinese bilingual).

Huang, T.K., Hsu, K.C., 1936. Mesozoic orogenic movements in the Pinghsiang coalfield, Kiangsi. Bulletin of Geology Society of China 16, 177–194.

Huang, D.H., Du, A.D., Wu, C.Y., Liu, L.S., Sun, Y.L., Zou, X.Q., 1996. Timing metallogenesis of molybdenum (copper) deposits in North China Platform: Re–Os ages for molybdenites and their implication. Mineral Deposits 15, 365–372 (in Chinese with English abstract).

Jahn, B., Wu, F., Chen, B., 2000. Massive granitoid generation in Centesl Asia: Nd isotope evidence and implication for continental growth in the Phanerozoic. Episodes 23, 82–92.

Jamieson, R.A., 1991. *P–T–t* paths of collisional orogeneses. Geologie Rundschau 180, 321–332.

Johson, T.W., Meinert, L.D., 1994. Au–Cu–Ag skarn and replacement mineralization in the McLaren deposit, New World district, Park County, Montana. Economic Geology 89, 969–993.

Kerrich, R., Goldfarb, R.J., Groves, D.I., Garwin, S., Jia, Y.F., 2000. The characteristics, origins and geodynamic settings of supergiant gold metallogenic provinces. Science in China. Series D 43, 1–68 (Suppl.).

Kroner, A., Zhang, G.W., Sun, Y., 1993. Granulites in the Tongbai area, Qinling Belt, China: geochemistry, petrology, single zircon geochronology, and implications for the tectonic evolution of eastern Asia. Tectonics 12, 245–255.

Lai, S.C., Zhang, G.W., Yang, R.Y., 2000. Identification of the island-arc magmatic zone in the Lianghe–Raofeng–Wuliba area, south Qinling and its tectonic significance. Science in China. Series D 43, 69–81 (Suppl.).

Lang, J.R., Baker, T., 2001. Intrusion-related gold systems: the present level of understanding. Mineralium Deposita 36, 477–489.

Li, T.D., 2002. Geology and metallogenic analysis of the Qiaoxiahala gold–copper–iron deposit in Fuyun county, Xinjiang. Geology and Prospecting 38 (1), 18–21 (in Chinese with English abstract).

Li, T.D., Xiao, X.C., 1996. Terrane structural analysis of the Tibet Plateau. The Lithospheric Architecture and the Development of the Tibet Plateau. Geological Publishing House, Beijing, pp. 6–20 (in Chinese).

Li, C.Y., Liu, Y.W., Zhu, B.Q., Feng, Y.M., Wu, H.Q., 1978. Tectonic evolution of the Qinling and Qilian Mountains. Contributions to 26th Internal Geological Congress, vol. 1. Geological Publishing House, Beijing, pp. 174–187 (in Chinese).

Li, H.Q., Xie, C.F., Chang, H.L., 1998. Geochronology of Mineralization of Nonferrous and Precious Metallic Deposits in Northern Xinjiang. Geological Publishing House, Beijing. 264 pp. (in Chinese with English abstract).

Li, C., Chen, Y.J., He, S.D., 2001. East Qinling–Dabieshan lithosphere delaminating age, mechanism and direction–petrological evidences and stipulation. Chinese Journal of Geochemistry 20, 59–72.

Lin, W., Faure, M., Sun, Y., Shu, L.S., Wang, Q.C., 2001. Compression to extension switch during the Middle Triassic orogeny of Eastern China: the case study of the Jiulingshan massif in the southern foreland of the Dabieshan. Journal of Asian Earth Sciences 20, 31–43.

Liu, J.G., Zhang, R.Y., Wang, X., Eide, E.A., Ernst, W.G., Maruyama, S., 1996. Metamorphism and tectonics of high-pressure and ultra-high-pressure belts in the Dabie–Sulu region, China. In: Yin, A., Harrison, T.M. (Eds.), The Tectonic Evolution of Asia. Cambridge University Press, Cambridge, pp. 300–344.

Lu, X., Yao, S., Li, Z., 2003. Characteristics and origin of fluid inclusions in the Tongshankou porphyry–skarn Cu–Mo deposit, Hubeu Province, P. R. China. ECROFI (European Current Research on Fluid Inclusions), Budapest, Hungary, p. 113.

Lu, X., Yao, S., 2004. Characteristics and origin of the fluid inclusions in the Tongshankou porphyry–skarn Cu (Mo) deposit, Hubei Province, China. 17th Australian Geological Convention, February, Hobart, Australia, p. 139.

Luan, S.W., 1987. Geology of Gold Deposits and Prospecting Methods. Sichuan Science and Technology Press, Chengdu. 550 pp. (in Chinese with English abstract).

Mao, J.W., Qiu, Y.M., Goldfarb, R.J., Zhang, Z.C., Garwin, S., Ren, F. S., 2002. Geology, distribution, and classification of gold deposits in the western Qinling belt, central China. Mineralium Deposita 37, 352–377.

Mao, J.W., Godlfarb, R.J., Seltmann, R., Wang, D.H., Xiao, W.J., Hart, C. (Eds.), 2003. Tectonic Evolution and Metallogeny of the Chinese Altay and Tianshan. International Association on the Genesis of Ore Deposits, Centre for Russian and Central Asian Mineral Studies. Natural History Museum, London. 282 pp.

Meinert, L.D., 1989. Gold skarn deposits–geology and exploration criteria. Economic Geology Monographs 6, 537–552.

Meinert, L.D., 1998. A review of skarns that contain gold. In: Lentz, D.R. (Ed.), Mineralized Intrusion-related Skarn Systems. Mineralogical Association of Canada Short Course Series, vol. 26, pp. 359–414.

Meinert, L.D., Hefton, K.K., Mayes, D., Tasiran, I., 1997. Geology, zonation, and fluid evolution of Big Gossan Cu–Au skarn deposit, Ertsberg district, Irian Jaya. Economic Geology 92, 509–534.

Meinert, L.D., Lentz, D.R., Newberry, R.J. (Eds.), 2000. Special Issue Devoted to Skarn Deposits. Economic Geology, vol. 95, pp. 1183–1184.

Meng, Q.R., Zhang, G.W., 1999. Timing of collision of the North and South China blocks: controversy and reconciliation. Geology 27, 123–126.

Meng, X.J., Hou, Z.Q., Gao, Y.F., Huang, W., Qu, X.M., Qu, W.J., 2003. Development of porphyry copper–molybdenum–lead–zinc ore-forming system in east Gandese belt, Tibet: evidence from Re–Os age of molybdenite in Bangpu copper polymetallic deposit. Mineral Deposits 22, 246–252 (in Chinese with English abstract).

Muller, D., 2002. Gold–copper mineralization in alkaline rocks. Mineralium Deposita 37, 1–3.

Pan, Y.M., Dong, P., 1999. The Lower Changjiang (Yangzi/Yangtze River) metallogenic belt, east central China: intrusion- and wall rock-hosted Cu–Fe–Au, Mo, Zn, Pb, Ag deposits. Ore Geology Reviews 15, 177–242.

Pirajno, F., Bagas, L., 2002. Gold and silver metallogeny of the South China Fold Belt: a consequence of multiple mineralizing events? Ore Geology Reviews 20, 109–126.

Pirajno, F., Jacob, R.E., Petzel, V.W.F., 1991. Distal skarn-type gold mineralization in the Central Zone of the Damara orogen, Namibia. In: Ladeira, E.A. (Ed.), Proceedings Brazil Gold'91. Balkema, Rotterdam, pp. 95–100.

Qin, D.J., 1996. Geological and geochemical study of skarn deposits in Shanxi Province. PhD thesis, Peking University, Beijing, China. 145 pp. (in Chinese).

Qiu, J.S., Wang, D.Z., Ren, Q.J., Fu, B., 1993. Physicochemical conditions and material sources for mineralization of the Shaxi porphyry copper (gold) deposit, Anhui Province. Journal of Nanjing University, Earth Science 5, 386–397 (in Chinese with English abstract).

Quan, H., Han, Q.Y., Ai, Y.F., Lin, Y.C., Wei, J.Y., 1992. The Features and Prospects of Metallogenesis of Polymetals, Gold and Silver in Yan–Liao Area of China. Geological Publishing House, Beijing. 134 pp. (in Chinese).

Robinson, P.T., Zhou, M.F., Hu, X.F., Reynolds, P., Bai, W.J., Yang, J. S., 1999. Geochemical constraints on the origin of the Hegenshan ophiolite, Inner Mongolia, China. Journal of Asian Earth Sciences 17, 423–442.

Rui, Z.Y., Huang, C.K., Qi, G.M., Xu, J., Zhang, H.T., 1984. Porphyry Copper (Molybdenum) Deposits of China. Geological Publishing House, Beijing. 350 pp. (in Chinese with English abstract).

Rui, Z.Y., Shi, L.D., Fang, R.H., 1994. Geology of Nonferrous Metallic Deposits in the Northern Margin of the North China

Block and Its Vicinity. Geological Publishing House, Beijing. 576 pp. (in Chinese).
Rui, Z.Y., Goldfarb, R.J., Qiu, Y.M., Zhou, T.H., Chen, R.Y., Pirajno, F., Yun, G., 2002. Palaeozoic–Early Mesozoic gold deposits of the Xinjiang Autonomous Region, northwestern China. Mineralium Deposita 37, 393–418.
Rui, Z.Y., Hou, Z.Q., Qu, X.M., Zhang, L.S., Wang, L.S., Liu, Y.L., 2003. Metallogenic epoch of Gangdese porphyry copper belt and uplift of Qinghai–Tibet Plateau. Mineral Deposits 22, 217–225 (in Chinese with English abstract).
Sawkins, F.J., 1984. Metal Deposits in Relation to Plate Tectonics. Springer-Verlag, Berlin. 325 pp.
Sengor, A.M.C., 1990. Plate tectonics and orogenic research after 25 years. Earth-Science Reviews 27, 1–207.
Sengor, A.M.C., Natal'in, B.A., 1996. Paleotectonics of Asia: fragments of synthesis. In: Yin, A., Harrison, T.M. (Eds.), The Tectonic Evolution of Asia. Cambridge University Press, Cambridge, pp. 486–640.
Shao, J.A., Zang, S.X., Mo, B.L., Li, X.B., Wang, B., 1995. Extension of orogenic belts and upwelling of asthenosphere: the example of Hingan–Mongolian orogenic belt. Chinese Science Bulletin 40, 50–56.
Sillitoe, R.H., 1972. A plate tectonic model for the origin of porphyry copper deposits. Economic Geology 67, 184–197.
Sillitoe, R.H., 1989. Gold deposits in western Pacific island arcs: the magmatic connection. Economic Geology Monographs 6, 274–291.
Sillitoe, R.H., 2002. Some metallogenic features of gold and copper deposits related to alkaline rocks and consequences for exploration. Mineralium Deposita 37, 4–13.
Song, S.H., 1994. Ore Deposits in China. Geological Publishing House, Beijing. 539 pp. (in Chinese).
Stein, H.J., Markey, R.J., Morgan, J.W., Du, A.D., Sun, Y., 1997. Highly precise and accurate Re–Os ages for molybdenite from the East Qinling molybdenum belt, Shaanxi province, China. Economic Geology 92, 827–835.
Sui, Y.H., Wang, H.H., Gao, X.L., Chen, H.Y., 2000. Ore fluid of the Tieluping silver deposit of Henan Province and its illustration of the tectonic model for collisional petrogenesis, metallogenesis and fluidization. Science in China. Series D 43, 108–121 (Suppl.).
Sun, W.D., Li, S.G., Chen, Y.D., Li, Y.J., 2002. Timing of synorogenic granitoids in the South Qinling, Central China: constraints on the evolution of the Qinling–Dabie orogenic belt. Journal of Geology 110, 457–468.
Sun, W.D., Xie, Z., Chen, J.F., Zhang, X., Chai, Z.F., Du, A.D., Zhao, J.S., Zhang, C.H., Zhou, T.F., 2003. Os–Os dating of copper and molybdenum deposits along the middle and lower reaches of the Yangtze River. Economic Geology 98, 175–180.
Tang, R.L., Luo, H.X., 1995. Geology of the Yulong Copper Ore Belt, Tibet. Geological Publishing House, Beijing. 454 pp. (in Chinese).
Torrey, C.E., Karjalainen, H., Joyce, P.J., Erceg, M., Stevens, M., 1986. Geology and mineralization of the Red Dome (Mungana) gold skarn deposit, North Queensland, Australia. In: MacDonald, A.J. (Ed.), Gold'86. Consult Internat. Inc., pp. 504–517.
Wang, D.Z., Ren, Q.J., Qiu, J.S., 1998. Geology and geochemistry of Mesozoic continental volcanism and related gold metallogenesis in East China. In: Hu, S.X., Wang, H.N., Wang, D.Z., Zhang, J.R. (Eds.), Geology and Geochemistry of Gold Deposits in East China. Science Press, Beijing, pp. 267–338 (in Chinese).
Wang, X.F., Metcalfe, I., Jian, P., He, L.Q., Wang, C.S., 2000. The Jinshajiang–Ailaoshan suture zone, China: tectonostratigraphy, age and evolution. Journal of Asian Earth Sciences 18, 675–690.
Wang, H.H., Chen, Y.J., Gao, X.L., 2001. The isotope geochemistry of the Kangshan gold deposit, Henan and its illustration of the CPMF model. Mineral Deposits 20, 190–198 (in Chinese with English abstract).
Wei, Y.F., Lu, Y.J., 1994. Gold Deposits of China. Seismological Press, Beijing. 329 pp. (in Chinese with English abstract).
Wen, J.M., Ji, H.B., 1996. Geological and Geochemical Study of the Baxi Gold Deposit, Sichuan. Research Report. Open Laboratory of Ore Geochemistry of CAS, Guiyang. 140 pp. (in Chinese).
Wilson, G.C., Rucklidge, J.C., Kilius, L.R., 1990. Sulphide gold content of skarn mineralization at Rossland, British Columbia. Economic Geology 85, 1252–1259.
Wong, W.H., 1927. Crustal movements and igneous activities in Eastern China since Mesozoic time. Bulletin of Geology Society of China 6 (1), 9–36.
Wong, W.H., 1929. The Mesozoic orogenic movements in Eastern China. Bulletin of Geology Society of China 8 (1), 33–44.
Wu, Y.C., 1990. A preliminary study on skarn gold deposits in the Lower Yangtze River district, Anhui. Symposium on Geology of Gold Deposits, vol. 1. Geological Publishing House, Beijing, pp. 193–205 (in Chinese).
Wu, Y.C., 1992. Three new genetic types of skarn Cu–Au deposits in the Lower Yangtze River district, Anhui. Proceedings of Symposium on 1985–1990 Advances in Geologic Science and Technology. Beijing Science and Technology Press, Beijing, pp. 359–363 (in Chinese).
Wu, Y.C., 1994. Metallogenic conditions and mineralizations of skarn gold deposits in the Lower Yangtze River district, Anhui. Symposium on Prospecting Directions and Methods for the Main Types of Gold Deposits. Geological Publishing House, Beijing, pp. 203–276 (in Chinese).
Xiao, W.J., Hou, Q.L., Li, J.L., Windley, B.F., Hao, J., Fang, A.M., Zhou, H., Wang, Z.H., Chen, H.L., Zhang, G.C., Yuan, C., 2000. Tectonic facies and the archipelago – accretion process of the West Kunlun, China. Science in China. Series D 43, 134–143 (Suppl.).
Xie, J.R., 1965. Guide to Geologic Exploration. Geological Publishing House, Beijing. 154 pp. (in Chinese).
Xu, G., Zhou, J., 2001. The Xinqiao Cu–S–Fe–Au deposit in the Tongling mineral district, China: synorogenic remobilization of a stratiform sulphide deposit. Ore Geology Reviews 18, 77–94.
Xu, J., Zhu, G., 1994. Tectonic models of the Tan-Lu fault zone, eastern China. International Geology Review 36, 771–784.
Yakubchuk, A., Seltmann, R.F., Shatove, V., 2003. Tectonics and metallogeny of the western part of the Altaid orogenic collage. In: Mao, J.W., Godlfarb, R.J., Seltmann, R., Wang, D.H., Xiao, W.J., Hart, C. (Eds.), Tectonic Evolution and Metallogeny of the Chinese Altay and Tianshan. International Association on the Genesis of Ore Deposits, Centre for Russian and Central Asian Mineral Studies. Natural History Museum, London, pp. 7–16.
Yang, X.S., Jin, Z.M., 2001. Studies on Rb–Sr and Sm–Nd isotope of Yadong leucogranite in Tibet: constraint on its age and source material. Geological Review 47, 300–307 (in Chinese with English abstract).
Ye, K., Cong, B., Ye, D., 2001. The possible subduction of continental material to depths greater than 200 km. Nature 407, 734–736.
Yin, A., Nie, S.Y., 1996. A Phanerozoic paliinspastic reconstruction of China and its neighboring regions. In: Yin, A., Harrison, T.M. (Eds.), The Tectonic Evolution of Asia. Cambridge University Press, Cambridge, pp. 442–485.

Yuan, X.C., 1996. Velocity structure of the Qinling lithosphere and mushroom cloud model. Science in China. Series D 39, 235–243.

Zaw, K., Peters, S.G., Cromie, P., Burret, C., Hou, Z., 2007. Nature, diversity of deposit types and Metallogenic relations of South China. Ore Geology Reviews 31, 3–47 (this volume). doi:10.1016/j.oregeorev.2005.10.006.

Zhai, Y.S., Yao, S.Z., Lin, X.D., Zhou, X.N., Wan, T.F., Jin, F.Q., Zhou, Z.G., 1992. Iron–Copper (Gold) Metallogeny of the Lower Yangtze River District. Geological Publishing House, Beijing. 325 pp. (in Chinese).

Zhai, X.M., Day, H.W., Hacker, B.R., You, Z.D., 1998. Palaeozoic metamorphism in the Qinling Orogen, Tongbai Mountains, central China. Geology 26, 371–374.

Zhang, D.Q., Sun, G.Y., 1988. Granitoids in East China. China University of Geoscience Press, Wuhan. 302 pp. (in Chinese).

Zhang, Z.M., Liou, J.G., Cloeman, R.G., 1984. An outline of the plate tectonics of China. Geological Society of America Bulletin 95, 295–312.

Zhang, G.W., Meng, Q.R., Yu, Z.P., Sun, Y., Zhou, D.W., Guo, A.L., 1996. Orogenesis and dynamics of the Qinling orogen. Science in China. Series D 39, 225–234.

Zhang, Y.N., Zhao, Y.M., Bi, C.S., 1998. Geology, zonation and fluid evolution of the Jilongshan Cu–Au skarn deposit, Hubei Province. Mineral Deposits 17, 365–368 (Suppl.) (in Chinese).

Zhang, J., Chen, Y.J., Shu, G.M., Zhang, F.X., Li, C., 2002. Compositional study of minerals within the Qinlingliang granite, Southwestern Shaanxi and discussions on the related problems. Science in China. Series D 45, 662–672.

Zhang, L.C., Shen, Y.C., Ji, J.S., 2003a. Characteristics and genesis of Kanggur gold deposit in the eastern Tianshan Mountains, NW China: evidence from geology, isotope distribution and chronology. Ore Geology Reviews 23, 71–90.

Zhang, Z.J., Chen, Y.J., Chen, H.Y., Bao, J.X., Liu, Y.L., 2003b. The petrochemical characteristics of the Hercynian granitoids in Tianshan and its geodynamic implications. Journal of Mineralogy and Petrology 23, 15–24 (in Chinese with English abstract).

Zhang, D.H., Xu, G.J., Liu, W., Golding, S., 2007. High salinity fluid inclusions in the Yinshan polymetallic deposit from the Dexing district, Jiangxi Province: their origin and significance for ore genesis. Ore Geology Reviews 31, 247–260 (this volume). doi:10.1016/j.oregeorev.2004.11.002.

Zhang, Y., Lin, G., Roberts, P.A., Ord, A., 2007. Numerical modelling of deformation and fluid flow in the Shuikoushan district, Hunan Province, South China. Ore Geology Reviews 31, 261–278 (this volume). doi:10.1016/j.oregeorev.2005.03.013.

Zhao, Z.P., 1986. Review of the 50th anniversary of the Indosinian Movement. Scientia Geologica Sinica (1), 7–15 (in Chinese).

Zhao, Y.M., Lin, W.W., Bi, C.S., Li, D.X., Jiang, C.J., 1990. Skarn Deposits of China. Geological Publishing House, Beijing. 354 pp. (in Chinese with English abstract).

Zhao, Y.M., Lin, W.W., Zhang, D.Q, Zhao, G.H., Chen, R.Y., 1992. Metasomatic Mineralization and Its Prospecting Significance. Beijing Science and Technology Press, Beijing. 156 pp. (in Chinese).

Zhao, Y.M., Lin, W.W., Bi, C.S., Zhang, Y.N., 1997. The distribution and geological characteristics of auriferous skarn deposits in China. Mineral Deposits 16, 193–203 (in Chinese with English abstract).

Zhao, Y.M., Zhang, Y.N., Bi, C.S., Guo, L., 1998. The discovery of the magnesioferrite from Au (Fe, Cu) magnesian skarn deposits and study of the magnesioferrite–magnesiomagnetite series. Acta Geologica Sinica 72, 382–391.

Zhao, Y.M., Zhang, Y.N., Bi, C.S., 1999. Geology of gold-bearing skarn deposits in the middle and lower Yangtze River Valley and adjacent regions. Ore Geology Reviews 14, 227–249.

Zhao, G., Wilde, S.A., Cawood, P.A., Sun, M., 2001. Archean blocks and their boundaries in the North China Craton: lithological, structural and *P–T* path constraints and tectonic evolution. Precambrian Research 107, 45–73.

Zheng, M.H., 1991. The elementary features of Qibaoshan Ca–skarns and Mg–skarns (associated ore deposit) in Hunan Province, China. Skarns — Their Genesis and Metallogeny. Theophrastus Publications S.A., Greece, pp. 325–340.

Zheng, M.H., Zhang, B., Zhang, Z.N., Zhou, Y.F., Lin, W.D., Shuai, D. Q., 1983. A preliminary classification on the types of gold deposits in China. Journal of Chengdu College of Geology (1), 27–42 (in Chinese with English abstract).

Zhou, D., Graham, S.A., 1996. The Songpan–Ganzi complex of the West Qinling Shan as a Triassic remnant ocean basin. In: Yin, A., Harrison, T.M. (Eds.), The Tectonic Evolution of Asia. Cambridge University Press, Cambridge, pp. 281–299.

Zhou, T.F., Yuan, F., Yue, S.C., Zhao, Y., 2000. Two series of copper–gold deposits in the middle and lower reaches of the Yangtze River area and the hydrogen, oxygen, sulphur and lead isotopes of their ore-forming hydrothermal systems. Science in China. Series D 43, 209–218 (Suppl.).

Zhou, T.H., Goldfarb, R.J., Phillips, G.N., 2002. Tectonics and distribution of gold deposits in China – an overview. Mineralium Deposita 37, 249–282.

Zhou, X.W., Li, X.Z., Li, X.M., 2002. Research on metallogenic model of the Laozuoshan gold deposit, Heilongjiang Province. Geology and Prospecting 38 (2), 18–22 (in Chinese with English abstract).

Zhou, T.F.., Yuan, F., Yue, S.C., Liu, X.D., Zhang, X., Fan, Y., 2007. Geochemistry and evolution of ore-forming fluids of the Yueshan Cu–Au skarn and vein-type deposits, Anhui Province, South China. Ore Geology Reviews 31, 279–303 (this volume). doi:10.1016/j.oregeorev.2005.03.016.

Zhu, X., 1953. Gold of China. China Commercial Publishing House, Shanghai. 69 pp. (in Chinese).

Zhu, M.X., 1992. Gold Mineralization in the Shuikoushan Gold Field, Hunan Province. Unpublished Research Report. Peking University, Beijing, 130 pp. (in Chinese).

Zhu, R.X., Yang, Z.Y., Wu, H.N., Ma, X.H., Huang, B.C., Meng, Z.F., Fang, D.J., 1998. Palaeomagnetic constraints on the tectonic history of the major blocks of China during the Phanerozoic. Science in China. Series D 41, 1–19 (Suppl.).